



A wavelet-based real-time fire detection algorithm with multi-modeling framework

Jaeseung Baek^a, Taha J. Alhindī^b, Young-Seon Jeong^{c,*}, Myong K. Jeong^{b,*}, Seongho Seo^d, Jongseok Kang^d, We Shim^d, Yoseob Heo^d

^a College of Business, Northern Michigan University, Marquette, MI 49855, USA

^b Department of Industrial and Systems Engineering, Rutgers University, Piscataway, NJ 08854, USA

^c Department of Industrial Engineering and Interdisciplinary Program of Arts & Design Technology, Chonnam National University, Gwangju 61186, South Korea

^d Division of Data Analysis, Korea Institute of Science and Technology Information, 66 Hoegiro, Dongdaemun-gu, Seoul 02456, South Korea



ARTICLE INFO

Keywords:

Feature selection
Fire detection algorithms
Fire sensing system
Fire hazards
Multi-resolution analysis
Real-time fire detection
Wavelet transforms
Wireless sensor network

ABSTRACT

This paper presents a wavelet-based real-time automated fire detection algorithm that takes into consideration the multi-resolution property of the wavelet transforms. Unlike conventional fire detection algorithms, which fail to capture temporal dependency within the fire sensor signals, the proposed wavelet-based features characterize temporal dynamics of chemical sensor signals generated from various types of fire, such as flaming, heating and smoldering fires. We propose a new feature selection technique based on types of fire to select the best features that can effectively discriminate between normal and various fire conditions. Then, a real-time fire detection algorithm with a multi-modeling framework is developed to effectively utilize the selected features and construct multiple fire detectors that are sensitive in monitoring various kinds of fires without prior knowledge. In addition, we develop a novel multi-sensor fusion system that incorporates various chemical sensors and collects an accurate and reliable fire dataset from different real-life fire scenarios in order to validate the performance of the proposed and existing fire detection algorithms. The experimental results with real-life and public fire data show that the proposed algorithm outperforms others with early detection time with a reasonable false alarm rate regardless of the type of fire.

1. Introduction

Fire disasters endanger human lives and the environment around the globe. Fire accidents are one of the most catastrophic threats that cause human injuries and fatalities as well as property loss. In 2021, local fire departments in the United States responded to 1,353,500 fires, resulting in 3,800 human deaths, 14,700 injuries, and \$15.9 billion in property damage (Shelby Hall, 2022). It is imperative to detect fires at the early stage since damages and casualties caused by fires grow exponentially over time (Lin et al., 2019). Therefore, several fire sensing techniques (systems) and fire detection algorithms that enable early warnings have been developed to minimize the consequences of fire accidents. However, they often yield an increased number of false alarms that may cause needless evacuation and emergency plans. For instance, an occurrence of false alarms in an aircraft is estimated to cost between \$30,000 and \$50,000 (Chen et al., 2007). Thus, real-time fire detectors

not only have to be fast but also reliable and accurate to reduce the loss of lives and infrastructure damages.

Fire sensing systems can be categorized into video and chemical sensor systems according to the type of data they measure (Fonollosa et al., 2018; Gaur et al., 2019). Video sensor systems use various equipment, such as charge-coupled device cameras and monitor fires based on pixel intensity (Majid et al., 2022; Sousa et al., 2019; Tao & Duan, 2023). However, several fire detectors based on video sensors have a time lag in the decision-making process because they are dealing with high-dimensional image data. Such detectors have difficulty identifying fires at the early stage since they only capture flame and smoke, which typically occur in a severe stage after the fire ignition (Gaur et al., 2019). On the contrary, chemical sensor systems utilize sensors sensitive to temperature, carbon monoxide (CO), carbon dioxide (CO₂), oxygen (O₂) and smoke particles, etc., produced by fires in the early stage that cannot be monitored from video-based sensing techniques (Dasari et al., 2020; Fonollosa et al., 2018; Milke et al., 2003). Besides, due to easy

* Corresponding authors.

E-mail addresses: jbaek@nmu.edu (J. Baek), t.alhindhi@rutgers.edu (T.J. Alhindī), young.jeong@jnu.ac.kr (Y.-S. Jeong), mjeong@soe.rutgers.edu (M.K. Jeong), shseo@kisti.re.kr (S. Seo), kangjs@kisti.re.kr (J. Kang), sw@kisti.re.kr (W. Shim), joseph87@kisti.re.kr (Y. Heo).

List of acronyms

CNN	Convolutional neural network
DWT	Discrete wavelet transform
EFST	Estimated fire starting time
FAR	False alarm rate
FSTA	Fire starting time accuracy
LSTM	Long short-term memory networks
NN	Nearest neighbor
PCA	Principal component analysis
PNN	Probabilistic neural network
SFFS	Sequential forward floating search
TBA	Thresholding-based algorithms
TFST	True fire starting time
WV-MMNN	Wavelet-based multi-modeling nearest neighbor
WV-PNN	Wavelet-based PNN

installation, low equipment cost and real-time monitoring capability, chemical sensor systems have been extensively used in various fields, such as aviation, naval, mining, and indoor buildings (Cestari et al., 2005; Chen et al., 2007; Milke et al., 2003; Muduli et al., 2019). Common fire detectors based on chemical sensor systems in the early days considered a single type of sensor (Li et al., 2019; Xu et al., 2021). Later, such detectors were expanded to include multiple types of sensors utilizing various kinds of sensor information which is critical to detect fires (Cestari et al., 2005; Fonollosa et al., 2018; Gottuk et al., 2002).

Although chemical sensor-based fire detectors have shown great potential, developing reliable and accurate fire detectors is challenging due to the unique characteristics of fire sensor data. First, chemical sensor signals behave differently based on fire types. Fire can be categorized into flaming, heating (cooking), and smoldering fires depending

on the substances or materials which undergo combustion (Baek et al., 2021; Bukowski et al., 2008; Cestari et al., 2005; Fonollosa et al., 2018; Gottuk et al., 2002). Flaming fire is the most common type of fire that occurs with visible flame and high temperature. In contrast, smoldering and heating fires occur without the generation of flame and produce low temperatures. Flaming fire is the most common type of fire that occurs with visible flame and high temperature. It is often caused by the combustion of a fuel source, such as gas, paper, or wood. On the other hand, smoldering fire happens when a heat source, such as cigarettes, home furniture, and cloth, begins to burn with insufficient oxygen to ignite into a flame (Nazir et al., 2022). Lastly, a heating (cooking) fire occurs in the kitchen when cooking oil or grease burns. The prolonged heating in cooking could cause oil or grease to overheat, potentially leading to a heating fire. Fig. 1 illustrates the progression from smoldering and heating fires (left) to flaming fires (right) in a polyurethane slab and cooking oil combustion experiment, respectively.

Moreover, Figs. 2 and 3 show an example of various sensor measurements under different fire types obtained from our fire sensing system described in Section 5. It is clearly shown in Fig. 2 that temperature rises abruptly at the initial stage under flaming. In contrast, the temperature rises gradually in smoldering and heating, making it challenging to detect fires at the early stage. Moreover, since it is hard to predict the fire type that may occur in the real world, selecting the critical sensors and making decision criteria for all fire types could be an issue when developing fire detectors. For instance, O₂ is not required for a smoldering fire to occur because such a fire could occur without the generation of flames. Thus, O₂ sensors are not necessary when monitoring smoldering fires. However, due to smoke produced during the combustion, dust intensity should be monitored to detect the fire in the early stage, as shown in Fig. 3(a). On the other hand, as demonstrated in Fig. 3(b), the O₂ sensor is more critical in detecting flaming fires because at least 10% of O₂ should be present in the air to generate flaming fires (Stauffer et al., 2007).

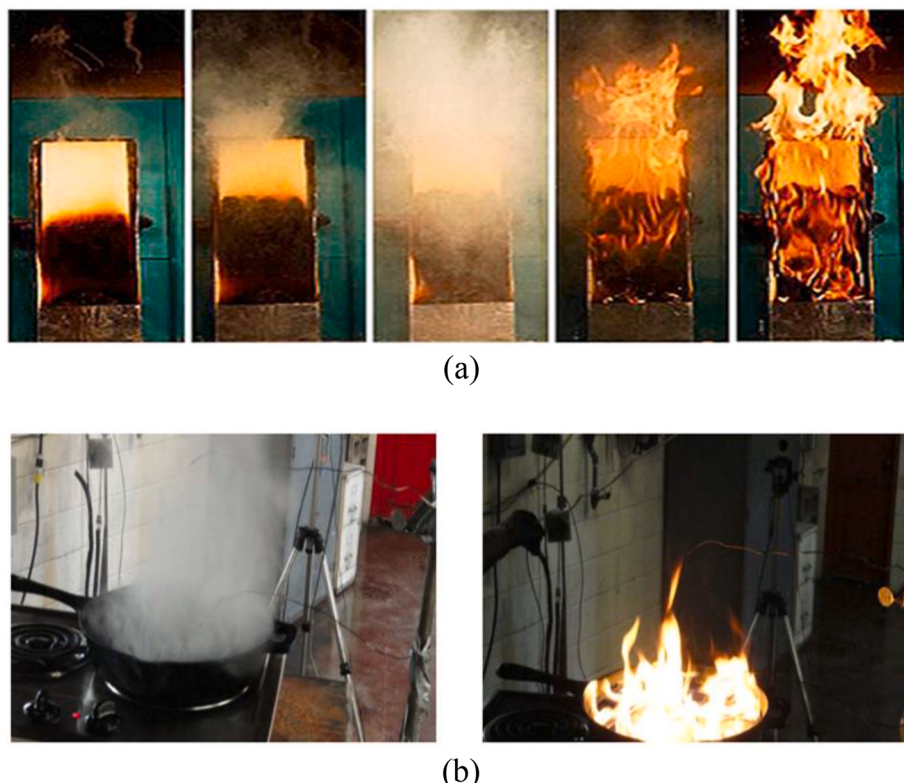


Fig. 1. Combustion experiments illustrating the transition from (a) smoldering to flaming (Santoso et al., 2019) and (b) cooking fire to flaming fire (Dinaburg & Guttuk, 2011).

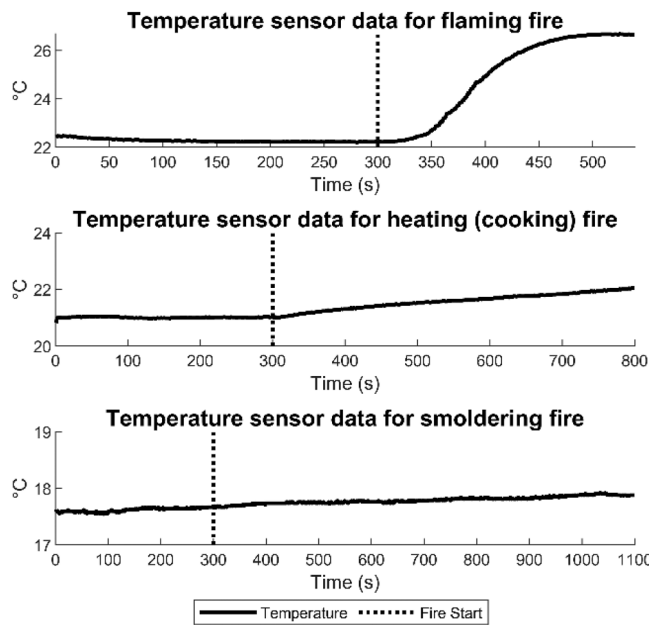


Fig. 2. Temperature sensor measurements of different fire types over time.

In this paper, we propose a novel fire detection approach to effectively detect various types of fires (i.e., flaming, heating, and smoldering fires). The main contribution of this paper is the development of a wavelet-based real-time fire detection approach that utilizes the multi-resolution property of the wavelet transforms in monitoring fires. Unlike existing approaches described in Section 2, which fail to consider complex patterns and temporal dynamics found in sensor signals that come from the various types of fires, limiting their applicability in diverse fire scenarios, the proposed approach can be useful in monitoring both dynamic and gradual changes in the sensor signals when a fire occurs by utilizing wavelet coefficients in the wavelet domain. In addition, the sequential forward floating search (SFFS) based feature selection method for multiple fire types (i.e., flaming, heating, and smoldering fires) is presented to select the wavelet-based features under consideration of different types of fire. Since sensor signals react differently according to fire types, several critical features, which are suitable for each type of fire and provide a better distinction between fire and non-fire conditions, should be chosen. Finally, a real-time fire detection algorithm with a multi-modeling framework is proposed to

construct multiple fire detection models by effectively utilizing selected features for different types of fire.

Furthermore, a novel multi-sensor fusion system is developed to collect accurate and reliable real-life fire datasets and validate the performance of the proposed algorithm. The existing fire datasets are collected under varying experimental settings, such as changing sensor positions and fire ignition times from one scenario to another, and they are obtained from limited sensors due to missing sensor measurements and different sampling intervals, making the performance comparison task challenging. In contrast, the proposed fire sensing system gathers diverse sensor measurements in real-time by incorporating multiple chemical sensors and obtains reliable sensor data under controlled experiments. The experimental results, obtained from the real-life data that is collected from the newly developed multi-sensor fusion system and the public data, show that the proposed approach provides a robust performance regardless of fire types in terms of earlier fire detection time and false alarm rate (FAR).

The remainder of this paper is organized as follows. In Section 2, we present a review of the relevant literature. Section 3 describes the proposed methodology and explores its properties. A performance study of public fire data is presented in Section 4, followed by a real-life case study using the multi-sensor fusion system in Section 5. Finally, Section 6 concludes with a brief summary and future study.

2. Related works

Several fire detection algorithms based on chemical sensor systems have been proposed over the years. Among them, thresholding-based fire detection algorithms that combine information from multiple sensors have been proposed by Cestari et al. (2005), Gottuk et al. (2002) and Fonollosa et al. (2018). Their algorithms employ multiple features, such as current sensor measurement and rate of measurement changes from predefined sensors. Since fire sensor signals tend to change after fire ignition, fire is detected when any of the observed features exceed thresholds that are selected based on engineering knowledge. Although the algorithms have the advantages of ease of implementation and fast computation, the main drawback is that they only utilize recent sensor measurements without considering sensor data from a longer period. Therefore, their approaches yield high false alarms when there exists fluctuation or noise in the signal. In addition, they are not appropriate in detecting different types of fire due to usage of predefined sensor information for all fire scenarios.

Instead of using current sensor measurements, multivariate statistical approaches have been proposed for fire monitoring by considering

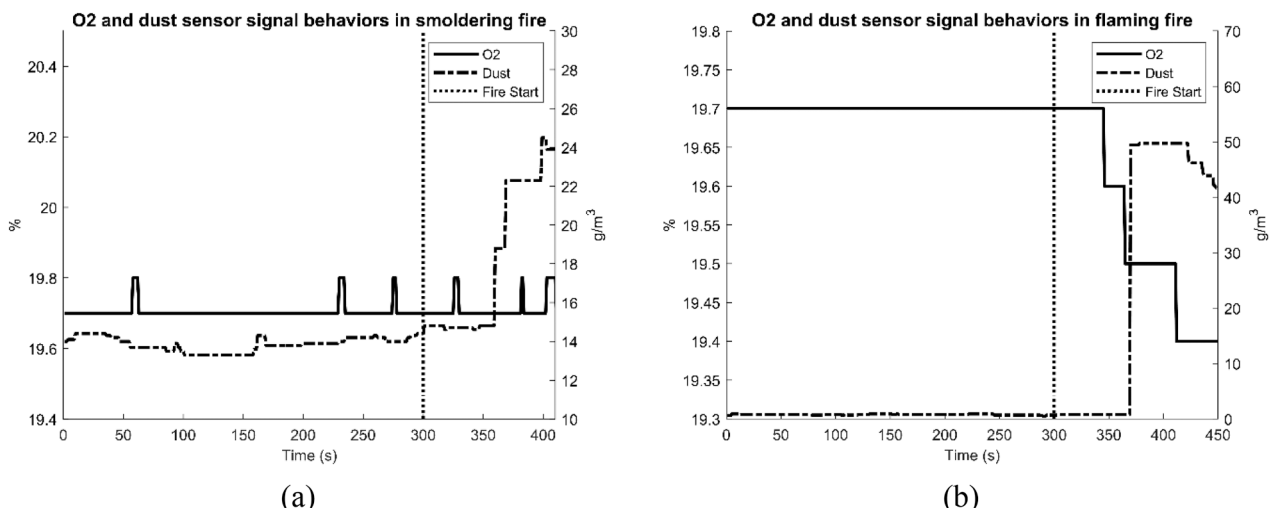


Fig. 3. O₂ and dust sensor reaction to (a) smoldering and (b) flaming fire.

the current and past sensor measurements for longer time periods (Cestari et al., 2005; JiJi et al., 2003) to capture long-term patterns, leading to more robust fire monitoring detection with low FAR. Sensor measurements from the past to current time points for different sensor types were used to obtain observations such that each observation contains total S features, where $S = \# \text{ of sensors} \times \# \text{ of time points}$. Principal component analysis (PCA) was applied to map original features into a lower-dimensional space, and then fires are monitored by using T^2 and Q statistics. An observation is classified as “fire” when Q or T^2 statistic exceeds the predefined threshold. However, since each sensor measurement is considered as a feature due to the vectorization of sensor measurements from all sensor types, the temporal dependency that exists in the sensor signals could be lost while using PCA. Moreover, the use of PCA may not be useful in high-dimensional sensor data because the successful implementation of PCA requires the number of observations to be greater than features (Croux & Ruiz-Gazen, 2005).

Moreover, the wavelet theory has been applied to chemical sensor-based fire detection methods because of its superior ability in “denoising” (Wang et al., 2013; Zheng et al., 2015). In current applications of wavelet techniques for fire detection, the wavelet method is primarily used to denoise sensor measurements. Training observations were obtained from the denoised sensor signals by wavelet denoising and included current and past sensor measurements, where each measurement was considered as a feature in an observation. Then, these observations were used to train machine learning classifiers, such as artificial neural network (ANN) models (Wang et al., 2013; Zheng et al., 2015). Wang et al. (2013) proposed the use of three different kinds of ANN models: the probabilistic neural networks (PNN), radial basis function (RBF), and backpropagation in fire monitoring. Zheng et al. (2015) applied a fuzzy RBF neural network to train the classification model for fire detection. However, during the wavelet denoising process, crucial information related to a fire event can be omitted or lost, resulting in poor performance in detecting fire. In addition, although neural networks have shown great potential in dealing with multivariate data, they fail to capture the temporal information among sensor data since these approaches consider each sensor measurement as a single feature.

Recently, advanced deep learning models based on convolution neural networks (CNN) have been applied to monitor fires (Chaoxia et al., 2020; Huang et al., 2022; Majid et al., 2022; Pincott et al., 2022; Tao & Duan, 2023). However, these approaches are based on video sensor systems, which utilize images of flames and smoke to detect fires. Thus, they may have limitations when it comes to early fire detection because the visual image of flame and smoke becomes apparent in the later stages of a fire after the fire has already ignited severely. Moreover, CNNs are typically designed to capture spatial relationships within the image data, which are not suited for time series data that contain temporal dependencies of sensor measurements collected in real-time. Recently, long short-term memory (LSTM) neural network models have been proposed in fire detection applications using chemical sensor signals (Benzekri et al., 2020; Dey et al., 2021; Wu et al., 2021). Since LSTM approaches are primarily designed for time-series data and their ability to model temporal dependencies, they can potentially overcome the drawbacks of using a CNN-based approach when dealing with chemical sensor data in fire detection applications. However, the performance of LSTM models heavily relies on the availability of large training datasets. Obtaining diverse datasets in fire detection applications could be challenging due to the limited amount of labeled fire data and the infrequent occurrence of fire events. Therefore, insufficient training data could hinder the model’s ability to generalize well and accurately detect fires.

3. Wavelet-based fire detection algorithm

This section proposes new features that integrate wavelet multi-resolution analysis for fire detection with a machine learning-based

feature selection method by considering different types of fire. Then, a novel fire detection approach based on a multi-modeling framework is proposed.

3.1. Multi-resolution wavelet technique for fire monitoring

In this study, a wavelet technique is applied to develop the novel fire detection approach by taking advantage of its multi-resolution property. Wavelet transform, which converts the signal in the time domain into approximated data with two basis functions, i.e., scaling (father) and wavelet (mother) functions in the wavelet domain, has been widely recognized as a powerful signal analysis tool in diverse applications. By using the two basis functions, an original signal $f(t)$ with fixed time length t_0 can be approximated as follows (Kwak et al., 2020; Vidakovic, 2009):

$$f(t) = \sum_{k=1}^{j_0} c_{j_0,k} \varnothing_{j_0,k}(t) + \sum_{j=j_0}^J \sum_{k=1}^{2^{j_0}} d_{j,k} \varphi_{j,k}(t) \quad (1)$$

where $2^{J+1} = t_0$, j_0 refers to the lowest decomposition level, $\varnothing_{j_0,k}(t)$ and $\varphi_{j,k}(t)$ represent scaling and wavelet functions. In addition, $c_{j_0,k}$ and $d_{j,k}$ are approximate and detailed coefficients, respectively, which are coefficients of basis functions $\varnothing_{j_0,k}(t)$ and $\varphi_{j,k}(t)$ where $j_0 \leq j \leq J$.

It is reasonable to assume that fire sensor measurements collected over time in normal operation, i.e., non-fire conditions, can be expressed as:

$$x(t) = f(t) + e(t), t \in \mathbb{R} \quad (2)$$

where $f(t)$ is a true fire sensor measurement and $e(t)$ are noises following independent and identically distributed (i.i.d.) normal distribution $N(0, \sigma^2)$. When a discrete wavelet transform (DWT) is applied to x , it is expressed by $d = Hx$, where d is the wavelet coefficients and H is the wavelet transform matrix. Thus, the original signal x can be reconstructed by the inverse DWT, such as $x = H^{-1}d$.

Assume that at time point t , a total of P multichannel sensor signals (i.e., temperature, CO, ionization, photoelectric and smoke obscuration), which consist of sensor measurements from current time t to past $t_0 - 1$ points (i.e., a total of t_0 sensor measurements collected at each second), are available as follows:

$$x_p = \{x_p(t - t_0 + 1), \dots, x_p(t)\}$$

where x_p represents p^{th} sensor signal for $p \in \{1, \dots, P\}$, which is comprised of the p^{th} sensor measurement $x_p(i)$ for $i \in \{t - t_0 + 1, \dots, t\}$. If $t_0 = 32$ and the Harr wavelet with the lowest decomposition level $j_0 = 1$ are applied (See Section 4.3 for the selection of t_0 and j_0), its DWT can be expressed as:

$$DWT[x_p] = \begin{bmatrix} c_{1,1}^p, c_{1,2}^p, d_{1,1}^p, d_{1,2}^p, d_{2,1}^p, d_{2,2}^p, d_{2,3}^p, d_{2,4}^p, \\ d_{3,1}^p, d_{3,2}^p, d_{3,3}^p, d_{3,4}^p, d_{3,5}^p, d_{3,6}^p, d_{3,7}^p, d_{3,8}^p, \\ d_{4,1}^p, d_{4,2}^p, d_{4,3}^p, d_{4,4}^p, d_{4,5}^p, d_{4,6}^p, d_{4,7}^p, d_{4,8}^p, \\ d_{4,9}^p, d_{4,10}^p, d_{4,11}^p, d_{4,12}^p, d_{4,13}^p, d_{4,14}^p, d_{4,15}^p, d_{4,16}^p \end{bmatrix}$$

where $DWT[x_p]$ is 1×32 vector that holds wavelet coefficients for x_p . In addition, $c_{j_0,k}^p$ is k^{th} approximation coefficient at the lowest decomposition level j_0 and $d_{j,k}^p$ is k^{th} detailed coefficient in scale j , for the p^{th} sensor signal. The detailed formulations of these wavelet coefficients are shown in Table 1. Note that wavelet coefficients are considered as features in the proposed algorithm, and we use the notation $s_{p,1}, \dots, s_{p,32}$, as denoted in the table, in preference to $c_{j_0,k}^p$ and $d_{j,k}^p$ for the components of $DWT[x_p]$.

Table 1

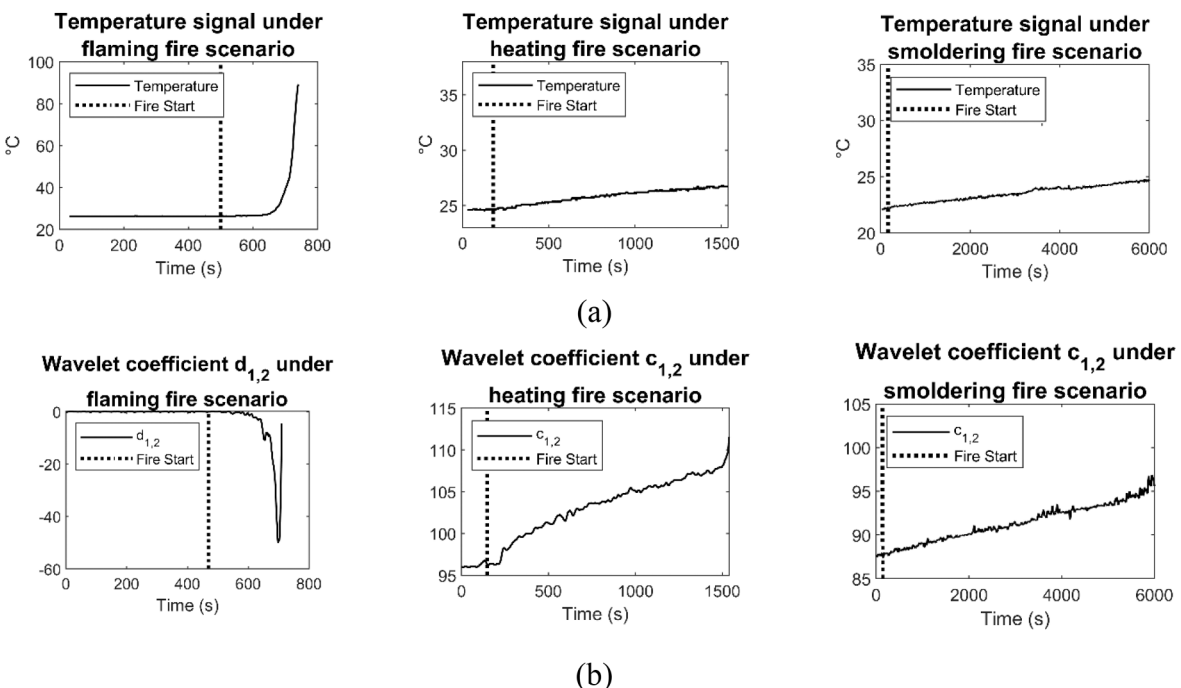
The equations of wavelet coefficients based on DWT.

Feature vector	Wavelet coefficient formulation	Feature vector	Wavelet coefficient formulation
$s_{p,1}$	$c_{1,1}^p = \frac{1}{\sqrt{16}} \left(\sum_{j=16}^{31} x_p(t-j) \right)$	$s_{p,2}$	$c_{1,2}^p = \frac{1}{\sqrt{16}} \left(\sum_{j=0}^{15} x_p(t-j) \right)$
$s_{p,3}$	$d_{1,1}^p = \frac{1}{\sqrt{16}} \left(\sum_{j=31}^{23} x_p(t-j) - \sum_{t=16}^{22} x_p(t-j) \right)$	$s_{p,4}$	$d_{1,2}^p = \frac{1}{\sqrt{16}} \left(\sum_{j=8}^{15} x_p(t-j) - \sum_{t=0}^7 x_p(t-j) \right)$
$s_{p,5}$	$d_{2,1}^p = \frac{1}{\sqrt{8}} \left(\sum_{j=28}^{31} x_p(t-j) - \sum_{j=24}^{27} x_p(t-j) \right)$	$s_{p,6}$	$d_{2,2}^p = \frac{1}{\sqrt{8}} \left(\sum_{j=20}^{23} x_p(t-j) - \sum_{j=16}^{19} x_p(t-j) \right)$
$s_{p,7}$	$d_{2,3}^p = \frac{1}{\sqrt{8}} \left(\sum_{j=12}^{15} x_p(t-j) - \sum_{j=8}^{11} x_p(t-j) \right)$	$s_{p,8}$	$d_{2,4}^p = \frac{1}{\sqrt{8}} \left(\sum_{j=4}^7 x_p(t-j) - \sum_{j=0}^3 x_p(t-j) \right)$
$s_{p,9}$	$d_{3,1}^p = \frac{1}{\sqrt{4}} \left(\sum_{j=30}^{31} x_p(t-j) - \sum_{j=28}^{29} x_p(t-j) \right)$	$s_{p,10}$	$d_{3,2}^p = \frac{1}{\sqrt{4}} \left(\sum_{j=26}^{27} x_p(t-j) - \sum_{j=24}^{25} x_p(t-j) \right)$
$s_{p,11}$	$d_{3,3}^p = \frac{1}{\sqrt{4}} \left(\sum_{j=22}^{23} x_p(t-j) - \sum_{j=20}^{21} x_p(t-j) \right)$	$s_{p,12}$	$d_{3,4}^p = \frac{1}{\sqrt{8}} \left(\sum_{j=18}^{19} x_p(t-j) - \sum_{j=16}^{17} x_p(t-j) \right)$
$s_{p,13}$	$d_{3,5}^p = \frac{1}{\sqrt{4}} \left(\sum_{j=14}^{15} x_p(t-j) - \sum_{j=12}^{13} x_p(t-j) \right)$	$s_{p,14}$	$d_{3,6}^p = \frac{1}{\sqrt{4}} \left(\sum_{j=10}^{11} x_p(t-j) - \sum_{j=8}^9 x_p(t-j) \right)$
$s_{p,15}$	$d_{3,7}^p = \frac{1}{\sqrt{4}} \left(\sum_{j=6}^7 x_p(t-j) - \sum_{j=4}^5 x_p(t-j) \right)$	$s_{p,16}$	$d_{3,8}^p = \frac{1}{\sqrt{4}} \left(\sum_{j=2}^3 x_p(t-j) - \sum_{j=0}^1 x_p(t-j) \right)$
$s_{p,17}$	$d_{4,1}^p = \frac{1}{\sqrt{2}} (x_p(t-31) - x_p(t-30))$	$s_{p,18}$	$d_{4,2}^p = \frac{1}{\sqrt{2}} (x_p(t-29) - x_p(t-28))$
$s_{p,19}$	$d_{4,3}^p = \frac{1}{\sqrt{2}} (x_p(t-27) - x_p(t-26))$	$s_{p,20}$	$d_{4,4}^p = \frac{1}{\sqrt{2}} (x_p(t-25) - x_p(t-24))$
$s_{p,21}$	$d_{4,5}^p = \frac{1}{\sqrt{2}} (x_p(t-23) - x_p(t-22))$	$s_{p,22}$	$d_{4,6}^p = \frac{1}{\sqrt{2}} (x_p(t-21) - x_p(t-20))$
$s_{p,23}$	$d_{4,7}^p = \frac{1}{\sqrt{2}} (x_p(t-19) - x_p(t-18))$	$s_{p,24}$	$d_{4,8}^p = \frac{1}{\sqrt{2}} (x_p(t-17) - x_p(t-16))$
$s_{p,25}$	$d_{4,9}^p = \frac{1}{\sqrt{2}} (x_p(t-15) - x_p(t-14))$	$s_{p,26}$	$d_{4,10}^p = \frac{1}{\sqrt{2}} (x_p(t-13) - x_p(t-12))$
$s_{p,27}$	$d_{4,11}^p = \frac{1}{\sqrt{2}} (x_p(t-11) - x_p(t-10))$	$s_{p,28}$	$d_{4,12}^p = \frac{1}{\sqrt{2}} (x_p(t-9) - x_p(t-8))$
$s_{p,29}$	$d_{4,13}^p = \frac{1}{\sqrt{2}} (x_p(t-7) - x_p(t-6))$	$s_{p,30}$	$d_{4,14}^p = \frac{1}{\sqrt{2}} (x_p(t-5) - x_p(t-4))$
$s_{p,31}$	$d_{4,15}^p = \frac{1}{\sqrt{2}} (x_p(t-3) - x_p(t-2))$	$s_{p,32}$	$d_{4,16}^p = \frac{1}{\sqrt{2}} (x_p(t-1) - x_p(t))$

throughout the paper.

The approximation coefficients represent the overall trends of sensor signals, and they can identify increasing or decreasing trends of the

signals. In contrast, the detailed coefficients catch the locality and details of the overall trends of the sensor signal, thus, providing better identification of sharp variations in the signals. Therefore, by using the

**Fig. 4.** Plots of (a) raw temperature sensor signals and (b) wavelet coefficients under flaming, heating, and smoldering fire scenarios.

characteristics of approximation and detailed wavelet coefficients, different types of fire could be effectively detected. Fig. 4(a) illustrates the temperature sensor signals obtained from flaming, smoldering, and heating fire scenarios, respectively. Although temperature sensor signal rises sharply in the early stages after fire ignition in the flaming fire scenario, signals from smoldering and heating fire scenarios rise slowly. Therefore, the abrupt change of signal from the flaming scenario can be well distinguished by wavelet coefficients at the detailed level (i.e., $d_{1,2}^p$), whereas an increasing trend of the sensor signals from both heating and smoldering scenarios can be better identified by using wavelets at the approximate level (i.e., $c_{1,2}^p$) as illustrated in Fig. 4(b).

3.2. Extraction of new features for fire detection

In Section 3.1, wavelet coefficients which contain multi-resolution information of fire sensor signals are presented. In order to build an effective fire detection model, however, it is essential to extract informative and robust features that can recognize the main characteristics of fire sensor signals. Therefore, in this study, several statistical features in the wavelet domain, such as mean, standard deviation, skewness, root mean square, form factor, crest-factor, energy, Shannon-entropy, log-energy entropy, and interquartile range, are also considered as new features. All features are individually applied to the wavelet coefficients at each scale and their detailed formulations are shown in Table 2.

Thresholding-based algorithms utilize features, such as current sensor values or rate of measurements change, which are denoted by $x_p(t)$ and $\frac{dx_p(t)}{dt} = \frac{x_p(t)-x_p(t-5)}{t-(t-5)}$, respectively (Cestari et al., 2005; Gottuk et al., 2002). Since fire sensor signals tend to change after fire ignition, using those features has been the basis of most traditional thresholding-based fire monitoring algorithms. Based on the combinations of wavelet coefficients presented in Table 1, features used in the thresholding-based algorithm can be obtained in the wavelet domain and can be utilized as new features. Each thresholding feature in the wavelet domain can be represented as follows:

$$s_{p,83} = x_p(t) = \frac{1}{4}c_{1,2}^p - \sum_{m=1}^4 \left(\frac{1}{\sqrt{2}} \right)^m d_{m,2^m}^p \quad (3)$$

$$s_{p,84} = \frac{dx_p(t)}{dt} = \frac{(d_{3,7}^p - d_{3,8}^p)}{10} - \frac{(d_{2,4}^p + d_{4,14}^p + d_{4,16}^p)}{5\sqrt{2}} \quad (4)$$

Thus, by applying the wavelet multi-resolution analysis to the fire sensor signal, 84 features that contain useful information for fire monitoring can be extracted for each sensor type.

3.3. Selection of the best features based on multiple fire types

As described in the previous section, several features can be extracted based on the wavelet multi-resolution analysis for fire detection. Given these features, the next task is to find the best set of features that can distinguish between non-fire and fire conditions.

Bhattacharyya distance is one of the popular measures that is used to quantify class separability (Baidari & Honnikoll, 2021; Kailath, 1967; Théodore et al., 2021). If measurements are gathered from multiple sensors, then multivariate time series data, which are a collection of a finite sequence of univariate sensor measurements, i.e., $\mathbf{X} = \{x_1, \dots, x_p, \dots, x_P\}$ where x_p refers to the p^{th} sensor signal with fixed time length, are used to represent the sensor data. When the DWT is applied and wavelet-features are extracted, we obtain $\mathbf{S} = \{s_1, \dots, s_p, \dots, s_P\}$, which is a collection of feature vectors where $s_p = \{s_{p,1}, \dots, s_{p,84}\}$. Let \mathbf{S}_F and \mathbf{S}_{NF} are feature vectors for fire and non-fire class, respectively, where $\mathbf{S}_F, \mathbf{S}_{NF} \in \mathbf{S}$. Assume that density functions of \mathbf{S}_F and \mathbf{S}_{NF} follow the Gaussian distribution, $N(\mu_F, \Sigma_F)$ and $N(\mu_{NF}, \Sigma_{NF})$, respectively. Then, we can compute the Bhattacharyya distance $B(\mathbf{S})$ as follows:

$$B(\mathbf{S}) = \frac{1}{8}(\mu_F - \mu_{NF})^T \left(\frac{\Sigma_F + \Sigma_{NF}}{2} \right)^{-1} (\mu_F - \mu_{NF}) + \frac{1}{2} \ln \frac{|\Sigma_F + \Sigma_{NF}|}{\sqrt{|\Sigma_F||\Sigma_{NF}|}} \quad (5)$$

where $\mu_F, \Sigma_F, \mu_{NF}$ and Σ_{NF} are means and covariances of \mathbf{S}_F and \mathbf{S}_{NF} . Note that the first term focuses on the distance between the means of fire and non-fire data, while the second term focuses on the difference between the covariance matrices of fire and non-fire data. The $B(\mathbf{S})$ produces a high value when the distance between two classes is large (i.e., when the two classes are distinct).

Based on the Bhattacharyya distance, the best feature subset among \mathbf{S} obtained from wavelet analysis was selected by using the SFFS method (Theodoridis & Koutroumbas, 2009). The objective of SFFS is to obtain the best subset of size l among the L features (i.e., $l \leq L$), which maximizes the class separability. It is worth noting that fire sensor signals react differently depending on the type of fire. In other words, in a certain type of fire, some sensors may be useful, but others may not. Therefore, appropriate features from different sensors should be selected

Table 2
Formulation of wavelet-based features.

Feature name	Feature vector	Detailed coefficients formulation ($j = 1, \dots, 4$)	Approximation coefficients formulation ($j_0 = 1$)
Mean	$s_{p,33}, \dots, s_{p,37}$	$s_{p,37-j} = \frac{1}{K} \sum_{k=1}^K d_{j,k}^p$	$s_{p,37} = \frac{1}{K} \sum_{k=1}^K c_{j_0,k}^p$
Standard deviation	$s_{p,38}, \dots, s_{p,42}$	$s_{p,42-j} = \frac{1}{K} \sum_{k=1}^K (d_{j,k}^p - s_{p,37-j})^2$	$s_{p,42} = \frac{1}{K} \sum_{k=1}^K (c_{j_0,k}^p - s_{p,37})^2$
Skewness	$s_{p,43}, \dots, s_{p,47}$	$s_{p,47-j} = \sqrt{\frac{1}{6K} \sum_{k=1}^K \left(\frac{d_{j,k}^p - s_{p,37-j}}{\sqrt{s_{p,42-j}}} \right)^3}$	$s_{p,47} = \sqrt{\frac{1}{6K} \sum_{k=1}^K \left(\frac{c_{j_0,k}^p - s_{p,37}}{\sqrt{s_{p,42}}} \right)^3}$
Root mean square	$s_{p,48}, \dots, s_{p,52}$	$s_{p,52-j} = \sqrt{\frac{1}{K} \sum_{k=1}^K d_{j,k}^p}$	$s_{p,52} = \sqrt{\frac{1}{K} \sum_{k=1}^K c_{j_0,k}^p}$
Form factor	$s_{p,53}, \dots, s_{p,57}$	$s_{p,57-j} = \frac{s_{p,37-j}}{s_{p,52-j}}$	$s_{p,57} = \frac{s_{p,37}}{s_{p,52}}$
Crest factor	$s_{p,58}, \dots, s_{p,62}$	$s_{p,62-j} = \frac{\max(d_{j,k}^p)}{s_{p,52-j}}$	$s_{p,62} = \frac{\max(c_{j_0,k}^p)}{s_{p,52}}$
Energy	$s_{p,63}, \dots, s_{p,67}$	$s_{p,67-j} = \sum_{k=1}^K d_{j,k}^p ^2$	$s_{p,67} = \sum_{k=1}^K c_{j_0,k}^p ^2$
Shannon entropy	$s_{p,68}, \dots, s_{p,72}$	$s_{p,72-j} = -\sum_{k=1}^K d_{j,k}^p \log(d_{j,k}^p)$	$s_{p,72} = -\sum_{k=1}^K c_{j_0,k}^p \log(c_{j_0,k}^p)$
Log-energy entropy	$s_{p,73}, \dots, s_{p,77}$	$s_{p,77-j} = \sum_{k=1}^K \log(d_{j,k}^p)$	$s_{p,77} = \sum_{k=1}^K \log(c_{j_0,k}^p)$
Interquartile range	$s_{p,78}, \dots, s_{p,82}$	$s_{p,82-j} = Q_3(d_{j,k}^p) - Q_1(d_{j,k}^p)$	$s_{p,82} = Q_3(c_{j_0,k}^p) - Q_1(c_{j_0,k}^p)$

Q_1 : First quartile, Q_3 : Third quartile.

depending on the fire type. In order to solve this issue, SFFS has been applied to S_F and S_{NF} for three types of fire scenarios (i.e., flaming, heating, and smoldering), and obtain three sets of best features that are useful for monitoring each fire type.

Let S^r denote feature vectors obtained from multichannel sensor signals for r^{th} type of fire, where $r \in \{1, \dots, 3\}$ (i.e., 1: flaming, 2: heating, 3: smoldering) and $S_{(k)}^r = \{s_1^r, s_2^r, \dots, s_k^r\}$, where $s_k^r \in S^r$ be the set of the best combination of k ($k \leq l$) features. In addition, assume that $Z_{(L-k)}^r$ refer to the complement of the set $S_{(k)}^r$. The algorithm is initialized by selecting a single feature, which calculates the best Bhattacharyya distance and obtains $S_{(1)}^r = \{s_{(1)}^r\}$. Then, the best subset $S_{(k+1)}^r$ ($k \geq 1$) comprised of $(k+1)$ features is formed by “borrowing” an element from $Z_{(L-k)}^r$. Then, return to the previously selected lower dimension subset to check whether the inclusion of this new element improves the class separability or not by conditionally excluding each feature in $S_{(k+1)}^r$. If it does, the new element is finally included in $S_{(k+1)}^r$. The algorithm runs until the predefined l features are selected. The detailed steps required for SFFS are explained in Algorithm 1.

Algorithm 1: SFFS based on multiple fire types

Given $S = \{s_1, \dots, s_p, \dots, s_p\}$ where $s_p = \{s_{p,1}, \dots, s_{p,84}\}$, we apply the following algorithm:

- 1: **for** $r = 1, \dots, 3$ **do**
- 2: **(Step 1. Initialization)**
- 3: **for** $p = 1, \dots, P$ **do**
- 4: **for** $k = 1, \dots, L$ **do**
- 5: Compute Bhattacharyya distance $B(s_{p,k})$
- 6: **for end**
- 7: **for end**
- 8: Select the feature with the best $B(s_{p,k})$ and obtain $S_{(1)}^r = \{s_{(1)}^r\}$
- 9: **(Step 2. SFFS)**
- 10: **for** $k = 1, \dots, l$ **do**
- 11: **(Step 2.1. Inclusion):** Choose the element s^+ that has the most effect from $Z_{(L-k)}^r$
- 12: Calculate $s^+ = \underset{z \in Z_{(L-k)}^r}{\operatorname{argmax}} B(\{S_{(k)}^r + z\})$
- 13: Set $S_{(k+1)}^r = \{S_{(k)}^r + s^+\}$ and $k = k + 1$
- 14: **(Step 2.2. Conditional Exclusion):** Find the feature s^- that has the least effect in $S_{(k)}^r$
- 15: Calculate $s^- = \underset{s \in S_{(k+1)}^r}{\operatorname{argmax}} B(\{S_{(k)}^r - s\})$
- 16: **if** $B(\{S_{(k)}^r - s^-\}) > B(S_{(k-1)}^r)$ **then**
- 17: Set $S_{(k-1)}^r = \{S_{(k)}^r - s^-\}$ and $k = k - 1$
- 18: Go to Step 2.2
- 19: **else**
- 20: Go to Step 2.1
- 21: **if end**
- 22: **for end**
- 23: **for end**

In order to obtain the best features through SFFS, public fire data described in Section 4 are implemented. Since fire types can be categorized into flaming, smoldering, and heating (cooking) fires as described in Section 1, we utilize three representative fire scenarios that can best describe each type of fire for the feature selection. In each scenario, fire and non-fire sensor data from 5 different sensors (i.e., sensor measurements from temperature, CO, ionization, photoelectric, and smoke obscuration sensors) installed in a near fire ignition place

were obtained for all time points. Table 3 summarizes the details of these scenarios, which include the type of fire, ignition material, and true fire starting time (TFST).

Based on the procedures described in Algorithm 1, a total of 15 features for each type of fire were chosen. Table 4 summarizes the selected features of different types of fire. In the table, $s_{p,j}$ represents the j^{th} wavelet feature from the p^{th} sensor, where $p \in \{1, \dots, 5\}$ (i.e., 1: temperature 2: CO 3: ionization 4: photoelectric 5: smoke obscuration sensor) and $j \in \{1, \dots, 84\}$. As shown in Table 4, features with approximation coefficients (i.e., $j = 37, 47, 52, 57, 67, 72, 77$) were chosen more often in both heating and smoldering scenarios, whereas the detailed coefficients features were selected more in the flaming scenario. This is true because the wavelet coefficients at the detailed level can distinguish the abrupt change of signal from the flaming scenario, and wavelet coefficients at the approximate level better identify an increasing trend of the sensor signals from both heating and smoldering scenarios, as discussed in Section 3.1.

Moreover, the features from the specific sensors that are critical to monitor a certain type of fire are selected more frequently by the proposed feature selection algorithm. It is known that temperature sensors are effective in monitoring flaming fires due to the high temperatures generated by the flames (Bukowski et al., 2008; Cestari et al., 2005). Moreover, the ionization sensor is more sensitive in detecting flaming and heating fires, whereas it shows poor performance in detecting smoldering fires (Cleary, 2011; Fonollosa et al., 2018). In contrast, CO and photoelectric sensors are more appropriate for detecting smoldering fires (Cleary, 2011; Fonollosa et al., 2018). As shown in Table 4, sensors that are more sensitive in detecting certain fire types are frequently chosen based on our feature selection technique. For instance, wavelet features from temperature, ionization, and smoke obscuration sensors (i.e., $s_{1,j}$, $s_{3,j}$ and $s_{5,j}$) are frequently selected in the flaming scenario. In addition, features from ionization sensors (i.e., $s_{3,j}$) and CO and photoelectric sensors (i.e., $s_{2,j}$ and $s_{4,j}$) are more chosen in heating and smoldering scenarios, respectively, and thus, clearly show the effectiveness of our algorithm.

3.4. Automated real-time fire detection algorithm with multi-modeling framework

In this section, we propose a wavelet-based multi-modeling nearest neighbor (WV-MMNN) fire detection algorithm that identifies current fire sensor observation as a “fire” or “non-fire”. The nearest neighbor (NN) method is one of the popular techniques that is used in various fields, such as the financial industry, cyber defense, and text mining (Bertolini et al., 2021; Gu et al., 2019; Hilal et al., 2021; Kumar et al., 2022). The NN anomaly detection is based on the idea that the NN distance of a normal observation is similar to the NN distance of the training data, while the NN distance of an abnormal observation exhibits some deviation from the normal observations.

Let X refer to multichannel sensor signals, which are a collection of a finite sequence of univariate sensor measurements, $X = \{x_1, \dots, x_p, \dots, x_P\}$ where $x_p = \{x_p(t-31), x_p(t-30), \dots, x_p(t)\}$ represent the p^{th} sensor signal from current time t to past 31 time points. Suppose that we have an N pre-labeled “non-fire” training data $X_{train} = \{X_1, \dots, X_n, \dots, X_N\}$, where $X_n = \{x_n^1, \dots, x_n^P\}$ represents n^{th} training data of multichannel sensor signals.

The proposed WV-MMNN fire detection algorithm includes Phases I and II. In Phase I, we construct multiple fire detection models for each type of fire from given N normal training data. The detailed procedures are explained in Algorithm 2. Initially, we apply DWT on X_{train} and calculate $S_{train} = \{S_1, \dots, S_n, \dots, S_N\}$, where S_n denotes wavelet feature vectors obtained from the n^{th} training data of multichannel sensor signals. Then, we obtain reduced training data with the selected wavelet feature set $S_{train,(l)}^r = \{S_{1,(l)}^r, \dots, S_{n,(l)}^r, \dots, S_{N,(l)}^r\}$ for r^{th} fire type, described

Table 3
Description of fire scenarios used for feature selection.

Scenario #	Fire type	Fire ignition material	TFST (s)
1	Smoldering	Chair	667
2	Heating	Cooking oil	853
3	Flaming	Mattress	729

Table 4

Feature selection results for different types of fire.

Fire type	Selected features														
	1	2	3	4	5	6	7	8	9	10	11	12	13	14	15
Flaming	S _{1,47}	S _{1,57}	S _{1,69}	S _{1,71}	S _{3,69}	S _{3,70}	S _{3,71}	S _{3,72}	S _{4,72}	S _{5,68}	S _{5,69}	S _{5,70}	S _{5,71}	S _{5,72}	S _{5,78}
Heating	S _{2,72}	S _{3,42}	S _{3,46}	S _{3,57}	S _{3,68}	S _{3,69}	S _{3,70}	S _{3,71}	S _{3,72}	S _{3,77}	S _{4,52}	S _{4,72}	S _{5,70}	S _{5,71}	S _{5,72}
Smoldering	S _{2,47}	S _{2,67}	S _{2,69}	S _{2,70}	S _{2,71}	S _{2,72}	S _{3,72}	S _{4,37}	S _{4,46}	S _{4,51}	S _{4,57}	S _{4,71}	S _{5,72}	S _{5,46}	S _{5,72}

in Section 3.3. Given $S_{train,(l)}^r$, NN distance D_n^r is calculated for $n \in \{1, \dots, N\}$, where D_n^r denotes the Euclidean distance between $S_{n,(l)}^r$ to the nearest neighbor in $S_{train,(l)}^r$. Then, sort D_n^r in increasing order and determine the threshold T_α^r from the p^{th} percentile value from the sorted D_n^r , where $p = 100(1 - \alpha)$ and α is the significance level.

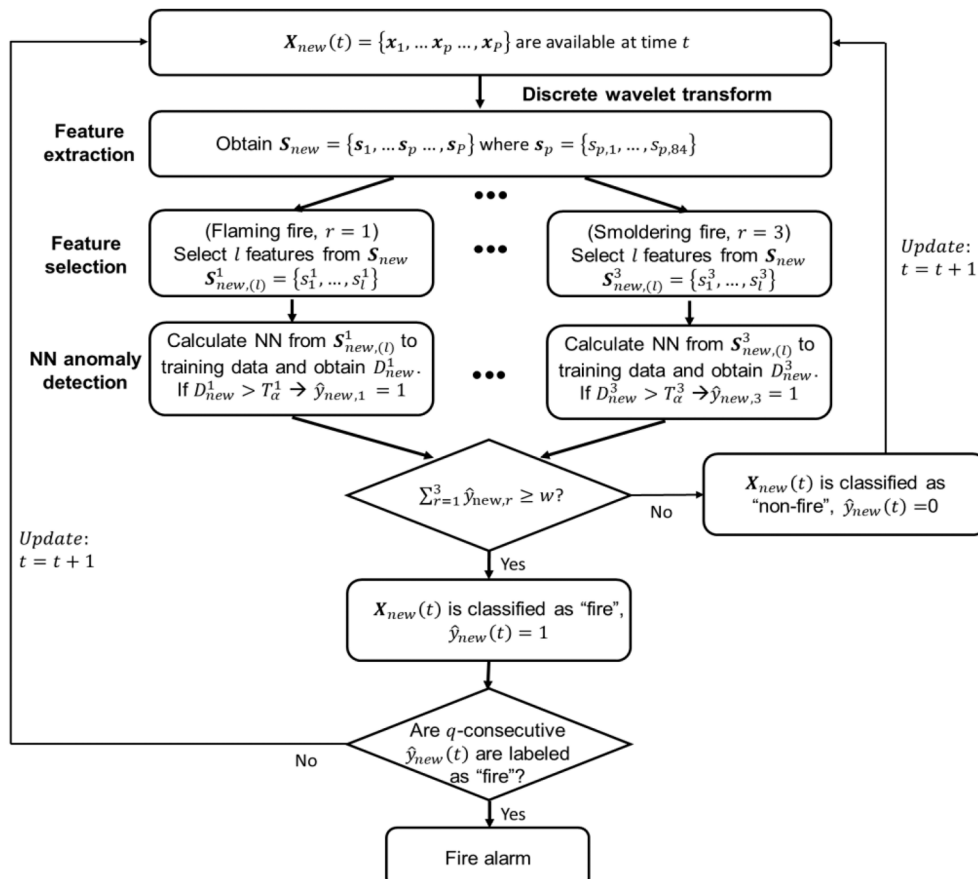
Algorithm 2: WV-MMNN fire detection algorithm: Phase I

Given N pre-labeled “non-fire” training data $X_{train} = \{X_1, \dots, X_n, \dots, X_N\}$, we apply the following algorithm:

- 1: Apply discrete wavelet transform to X_{train}
- 2: Extract wavelet features and obtain $S_{train} = \{S_1, \dots, S_n, \dots, S_N\}$
- 3: **for** $r = 1, \dots, 3$ **do**
- 4: Obtain reduced data with l selected features
 $S_{train,(l)}^r = \{S_{1,(l)}^r, \dots, S_{n,(l)}^r, \dots, S_{N,(l)}^r\}$ where $S_{n,(l)}^r = \{s_{n,1}^r, s_{n,2}^r, \dots, s_{n,l}^r\}$ and l is the predefined best feature number
- 5: **for** $n = 1, \dots, N$ **do**
- 6: Calculate NN distance D_n^r
- 7: **end for**
- 8: Rank the calculated D_n^r in an increasing order
- 9: Obtain the threshold T_α^r from p^{th} percentile value from the sorted D_n^r where $p = 100(1 - \alpha)$ and α is the significance level
- 10: **end for**

Subsequently, in Phase II, the objective is to decide whether the new observation is normal (i.e., non-fire condition) or abnormal (i.e., fire condition) based on the three learned models from phase I. At time t , assume that a multichannel sensor signal $X_{new}(t) = \{x_1, \dots, x_p, \dots, x_p\}$ is available. First, we follow the same procedures in Phase I and calculate D_{new}^r for $r \in \{1, 2, 3\}$. Then, if $D_{new}^r > T_\alpha^r$, predicted class label for each type of fire, $\hat{y}_{new,r}$, is labeled as 1; otherwise, $\hat{y}_{new,r}$ is labeled as 0.

It is worth noting that three predicted labels are obtained based on the proposed algorithm since we are considering three different fire detection models. Hence, in order to determine \hat{y}_{new} for $X_{new}(t)$, the predicted labels for each type of fire $\hat{y}_{new,r}$ should be combined appropriately. Therefore, we combine decision rules from fire detection models by using “ w -out-of-3: fire detector voting rule”. In the proposed voting rule, each fire detection model is considered as a voter and the new observation is considered as a “fire” when w or more models label the new observation as “1”. In other words, $X_{new}(t)$ is labeled as “fire” (i.e., $\hat{y}_{new} = 1$) when $\sum_{r=1}^3 \hat{y}_{new,r} \geq w$. Otherwise, we classify $X_{new}(t)$ as “non-fire” (i.e., $\hat{y}_{new} = 0$). In addition, during the real-time monitoring stage, a fire starting time is estimated, and a fire alarm is raised when

**Fig. 5.** An overview of Phase II in the WV-MMNN fire detection algorithm.

q -consecutive $\hat{y}_{new}(t)$ are labeled as “fire” to reduce false alarms. An overview of Phase II in the WV-MMNN fire detection algorithm is explained in Fig. 5.

4. Performance study

In this section, we demonstrate the performance of the proposed fire monitoring method in various fire scenarios. The performance of the proposed method is compared with existing fire monitoring approaches, and its results are discussed.

4.1. Fire data description

Public data from home smoke alarm tests gathered by the National Institute of Standards and Technology (NIST) was used to conduct the performance study. They manufactured residential homes and conducted various fire experiments by changing fuel sources (chairs, mattresses, and cooking oil) and ignition locations (bedroom, living room, and kitchen) (Bukowski et al., 2008). For consistent experimental settings, non-fire and 13 fire scenarios that share the same sensor types (i.e., Temperature, CO, ionization, photoelectric, and smoke obscuration sensors) and sensor locations (i.e., bedroom, kitchen, living area) are chosen. From these scenarios, 3 representative scenarios for each fire type (i.e., flaming, smoldering, and heating) are chosen to determine the best features using the feature selection approach presented in Section 3.3. Then 1000 training observations, which are randomly selected from the non-fire scenario, are utilized to construct the decision boundary of the proposed WV-MMNN using Algorithm 2, described in Section 3.4. Lastly, the remaining 10 scenarios are reserved as testing scenarios to evaluate the performance. Table 5 summarizes the details of these scenarios that include the type of fire, ignition material, location of fire, and TFST. Locations of the fire ignition place and sensors are shown in Fig. 6 (Bukowski et al., 2008), marked by red and black circles, respectively. Temperature, CO, ionization, photoelectric, and smoke obscuration sensors were deployed in the experiment (Cestari et al., 2005; Gottuk et al., 2002; Zheng et al., 2015). Examples of sensor signals obtained from different locations under fire scenarios are shown in Fig. 7. In the figure, sensor signals installed in the bedroom, kitchen, and hallway are shown in solid, dashed, and dotted-dashed line types, respectively, as well as the fire starting time is shown by a dotted vertical line.

4.2. Performance comparison

A few existing fire monitoring algorithms were selected in order to compare the performance with the proposed method. Existing fire monitoring algorithms for performance comparison include six thresholding-based algorithms (TBA) (Cestari et al., 2005; Fonollosa et al., 2018; Gottuk et al., 2002), multivariate statistical-based algorithms (Ji Ji et al., 2003), a wavelet-based PNN (WV-PNN) algorithms (Wang et al., 2013), and LSTM recurrent neural network algorithm (Benzekri et al., 2020). In the experiment, we obtained sensor measurements from a past time $t - 31$ to the current time t for 15 sensors

Table 5
Description of experiment scenarios.

Scenario #	Fire type	Fire ignition material	Fire location	TFST (s)
1	Smoldering	Mattress	Bedroom	467
2	Heating	Cooking oil	Kitchen area	178
3	Heating	Cooking oil	Kitchen area	500
4	Flaming	Chair	Living area	500
5	Flaming	Chair	Living area	500
6	Flaming	Chair	Living area	500
7	Flaming	Mattress	Bedroom	238
8	Flaming	Mattress	Bedroom	500
9	Flaming	Mattress	Bedroom	500
10	Flaming	Mattress	Bedroom	500

(5 sensors \times 3 locations) for each observation in multivariate statistical-based and WV-PNN as well as the proposed algorithm. We set $q = 10$ for all algorithms throughout the experiment based on Wang et al. (2013).

The TBA utilizes a combination of features obtained from different types of sensors at the current time t . The features considered in these algorithms were current sensor measurement of temperature, CO, ionization, photoelectric and rate of temperature changes, which are denoted by $x_{Temp}(t)$, $x_{CO}(t)$, $x_{Ion}(t)$, $x_{Pho}(t)$ and $\frac{dx_{Temp}(t)}{dt}$, respectively, where $\frac{dx_{Temp}(t)}{dt} = \frac{x_{Temp}(t) - x_{Temp}(t-5)}{t-(t-5)}$. The current observation is considered as “Fire” if any of these features exceed the predefined thresholds. The sensor types and decision-making criteria in each TBA are summarized in Table 6. For the multivariate statistical-based algorithms, Q -and T^2 -statistics were used, and their upper control limit was set to 99% and 99.9% (Ji Ji et al., 2003). The WV-PNN algorithm applies the wavelet method for denoising the raw sensor signals and uses PNN for monitoring the fire. The structure of the PNN consists of 480 neurons (i.e., 32 seconds \times 3 locations \times 5 sensors) in the 1st layer, 2 hidden layers and a single neuron in the output layer (Mohebali et al., 2020). The network was pretrained by using training observations from both fire and non-fire conditions. In addition, using the same training dataset of PNN, we trained an LSTM network using the Adam optimizing algorithm (Soydaner, 2020) consisting of 150 hidden neurons in the LSTM hidden layer with minibatch size and maximum epochs set to 50. In order to evaluate the performance of the proposed algorithm, we applied 15 features chosen from Section 3.2 to each location and obtained 45 features (i.e., 15 features \times 3 locations) for each type of fire. Then, thresholds for WV-MMNN are selected by setting $\alpha = 0.001$ for each type of fire.

The performance of all algorithms was evaluated by two performance measures. The FAR deals with false positive alarms that are detected by a given algorithm up to the time when the actual fire starts. FAR is calculated by:

$$FAR = \left[\frac{1}{TFST - 1} * \sum_{t=1}^{TFST-1} |\hat{y}(t) - y(t)| \right] \quad (6)$$

where $y(t)$ is the true observation label at time t and $\hat{y}(t)$ is the predicted observation label at time t , where $y(t), \hat{y}(t) \in \{0, 1\}$. The second performance measure is the fire starting time accuracy (FSTA), which is the absolute difference between the TFST to the estimated fire starting time (EFST), which is a detection time of a fire event obtained from the algorithm, for a given scenario. The FSTA for a testing scenario is given by:

$$FSTA = |TFST - EFST|. \quad (7)$$

Table 7 summarizes the performance comparison between the proposed approach and the existing fire detection approaches. FSTA for flaming fire scenarios appears to be short due to the apparent behavior of the sensor measurements after the fire ignition. In contrast, sensor signals from smoldering fires rise slowly or remain unchanged. These signals display patterns similar to those observed in normal conditions, making it challenging to detect fires during the early stages and resulting in longer FSTA. As shown in Table 7, the proposed fire monitoring approach is superior to the existing monitoring approaches in terms of EFST and FSTA with reasonable FAR.

The results show that the TBAs show high sensitivity in detecting fires when the fire sensor signals fluctuate or have noise since the decision is made based on current or recent time point measurements. Thus, false alarms are very common in some of these algorithms that produce low FSTA. In addition, the performance of TBAs is not robust to different kinds of fire because of deploying the same sensor types and thresholds for all scenarios. Therefore, the algorithm that performs well in one fire type yields high EFST and FSTA in others. Q-statistic, T^2 -statistic and WV-PNN show poor performance in fire detection since each sensor measurement is considered as an independent feature in these algorithms, and those algorithms fail to consider the temporal

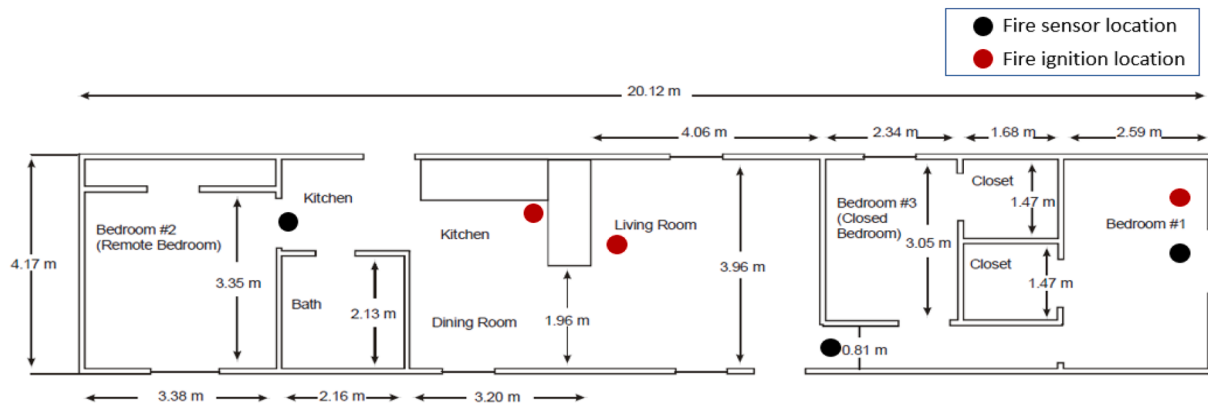


Fig. 6. Location of fire ignition and sensors (Bukowski et al., 2008).

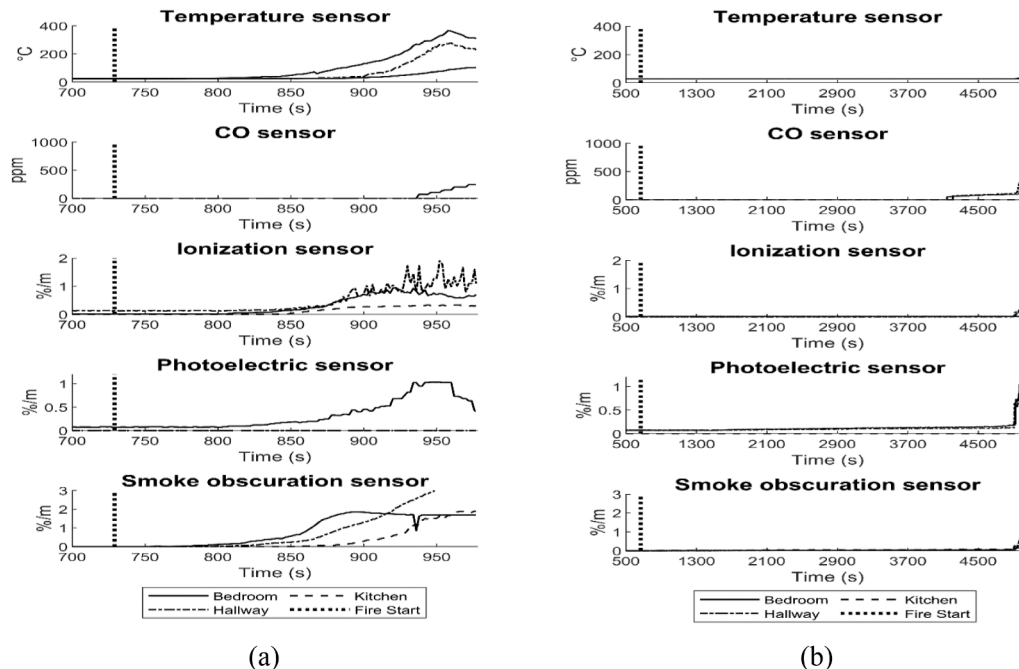


Fig. 7. Recorded sensor signals of all sensors under the (a) flaming scenario and (b) smoldering scenario.

Table 6
Sensor types and decision-making criteria of each TBA.

Algorithm #	Sensor types	Decision-making criteria
1	Temperature and CO	$\frac{dx_{Temp}(t)}{dt} > 0.07 \text{ } ^\circ\text{C}$ or $x_{CO}(t) > 2 \text{ ppm}$
2	Temperature, CO and ionization	$\frac{dx_{Temp}(t)}{dt} > 0.2 \text{ } ^\circ\text{C}$ or $x_{CO}(t) > 17 \text{ ppm}$ or $x_{Ion}(t) > 0.15\%/\text{m}$
3	CO and ionization	$x_{Ion}(t) * (x_{CO}(t) - 5) > 0.15$ or $x_{CO}(t) > 16 \text{ ppm}$ or $x_{Ion}(t) > 0.15\%/\text{m}$
4	Temperature and photoelectric	$\frac{dx_{Temp}(t)}{dt} > 0.2 \text{ } ^\circ\text{C}$ or $x_{Pho}(t) > 0.5\%/\text{m}$
5	Ionization and photoelectric	$x_{Ion}(t) > 0.15\%/\text{m}$ or $x_{Pho}(t) > 0.5\%/\text{m}$
6	CO and ionization	$x_{CO}(t) * x_{Ion}(t) > 10$

relationship among a sensor signal. In addition, dimension reduction and denoising the sensor data based on PCA and wavelet denoising, respectively, result in the loss of crucial information related to a fire event. Therefore, they are insensitive in detecting various signal patterns, such as dynamic or gradual signal changes that occur in the sensor data, and achieve poor performance in detecting fires.

On the contrary, the proposed approach outperforms the existing fire monitoring approaches for the following reasons. Firstly, compared to the existing algorithms, which fail to capture various temporal patterns contained in sensor signals due to the usage of each sensor measurement as a single feature, the proposed wavelet feature based on both detailed and approximation coefficients can effectively capture different signal patterns in various fire types. The sharp change in sensor signals from a flaming fire can be well distinguished by detailed coefficients, whereas an increasing trend of sensor signals from both heating and smoldering fire can be better identified by using approximation coefficients. Therefore, in the feature selection stage, wavelet features with detailed coefficients are selected more frequently in a flaming scenario, and features with approximation coefficients are often chosen in both heating and smoldering scenarios. The LSTM neural network can also capture temporal dependencies in the sensor data and performs better

Table 7Performance of existing and proposed fire detection algorithm on NIST fire data.^a

Scenario #	TFST	TBA 1			TBA 2			TBA 3		
		EFST (s)	FSTA (s)	FAR (%)	EFST (s)	FSTA (s)	FAR (%)	EFST (s)	FSTA (s)	FAR (%)
1	467	3810	3343	0.43	3821	3354	0.00	3825	3358	0.00
2	178	1605	1427	0.00	858	680	0.00	42	136	81.92
3	500	1725	1225	3.81	1718	1218	0.00	1241	741	0.00
4	500	585	85	0.00	638	138	0.00	587	87	0.00
5	500	629	129	3.81	636	136	0.00	591	91	0.00
6	500	236	264	6.01	644	144	0.40	600	100	0.00
7	238	319	81	0.00	331	93	0.00	287	49	0.00
8	500	569	69	4.61	586	86	0.00	626	126	0.00
9	500	563	63	0.20	569	69	0.00	603	103	0.00
10	500	567	67	4.81	590	90	0.00	622	122	0.00
Median			107.00	2.12		137.00	0.00		112.50	0.00
Average			675.30	2.37		600.80	0.04		491.30	8.19
Scenario #	TFST	TBA 4			TBA 5			TBA 6		
		EFST (s)	FSTA (s)	FAR (%)	EFST (s)	FSTA (s)	FAR (%)	EFST (s)	FSTA (s)	FAR (%)
1	467	42	425	93.13	3830	3363	0.00	3986	3519	0.00
2	178	1779	1601	0.00	858	680	0.00	1779	1601	0.00
3	500	1326	826	0.00	1530	1030	0.00	1864	1364	0.00
4	500	582	82	0.80	638	138	0.00	733	233	0.00
5	500	652	152	0.00	636	136	0.00	717	217	0.00
6	500	676	176	0.40	644	144	0.00	723	223	0.00
7	238	42	196	86.50	342	104	0.00	444	206	0.00
8	500	586	86	0.00	659	159	0.00	851	351	0.00
9	500	569	69	0.00	623	123	0.00	654	154	0.00
10	500	590	90	0.00	633	133	0.00	633	133	0.00
Median			164.00	0.00		141.00	0.00		228.00	0.00
Average			370.30	18.08		601.00	0.00		800.10	0.00
Scenario #	TFST	Q-statistic			T ² -statistic			WV-PNN		
		EFST (s)	FSTA (s)	FAR (%)	EFST (s)	FSTA (s)	FAR (%)	EFST (s)	FSTA (s)	FAR (%)
1	467	3985	3518	0.00	3828	3361	0.00	3985	3518	0.00
2	178	1778	1600	0.00	1599	1421	0.00	1575	1397	0.00
3	500	1842	1342	0.00	1735	1235	0.00	1421	921	0.00
4	500	692	192	0.00	651	151	0.00	682	182	0.00
5	500	716	216	0.00	651	151	0.00	694	194	0.00
6	500	722	222	0.00	655	155	0.00	696	196	0.00
7	238	354	116	0.00	318	80	0.00	418	180	0.00
8	500	598	98	0.00	40	460	100.00	676	176	0.00
9	500	587	87	0.00	40	460	11.73	633	133	0.00
10	500	607	107	0.00	592	92	0.00	632	132	0.00
Median			204.00	0.00		307.50	0.00		188.00	0.00
Average			749.80	0.00		756.60	11.17		702.90	0.00
Scenario #	TFST	LSTM			WV-MMNN					
		EFST (s)	FSTA (s)	FAR (%)	EFST (s)	FSTA (s)	FAR (%)			
1	467	1249	782	0.00	1205	738	0.00			
2	178	1210	1032	0.00	317	139	1.36			
3	500	1336	836	0.00	777	277	4.26			
4	500	635	135	0.00	579	79	1.49			
5	500	661	161	0.00	588	88	2.56			
6	500	664	164	0.00	593	93	6.18			
7	238	319	81	0.00	283	45	2.42			
8	500	650	150	0.00	561	61	5.54			
9	500	625	125	0.00	541	41	1.49			
10	500	632	132	0.00	577	77	0.21			
Median			155.50	0.00		83.50	1.95			
Average			359.80	0.00		163.80	2.55			

^a The numbers in bold indicate the best FSTA performance.

than the existing algorithms mentioned above. However, the limited availability of abnormal data and the wide variety of fire types hinder the model's ability to obtain a generalized model and accurately detect various types of fires as deep-learning models require a larger training dataset to successfully train and optimize the hyperparameters in the prediction models (Oyedare & Park, 2019).

Furthermore, the proposed feature selection algorithm chooses features from different sensors depending on the types of fire by adaptively selecting sensor information that is more sensitive in detecting a specific type of fire. Lastly, the proposed WV-MMNN fire detection algorithm

effectively combines multiple feature sets and builds multiple fire detectors that are suitable for monitoring various kinds of fires without prior knowledge of the fire type that may occur. Therefore, the WV-MMNN algorithm provides an earlier EFST and robust performance regardless of the type of fire compared to existing algorithms, as demonstrated in Table 7.

4.3. Effect of the parameters on the performance

In this section, we discuss the effect of parameters involved in the

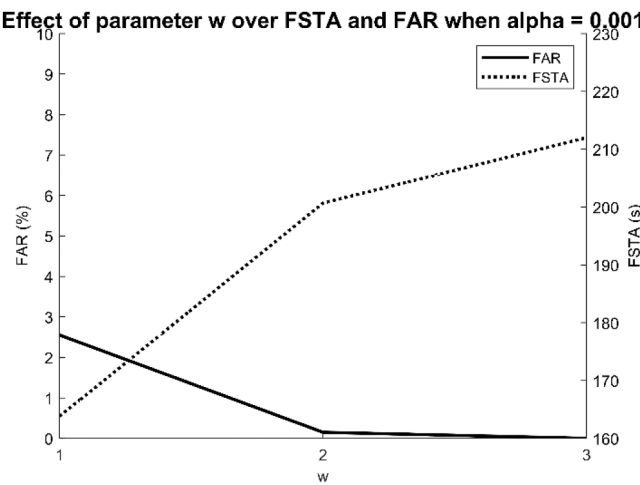


Fig. 8. Effect of parameter w on FSTA and FAR.

proposed algorithm. In the WV-MMNN algorithm, the parameter w , t_0 and j_0 should be prespecified before evaluating the performance.

In the WV-MMNN algorithm, the parameter w decides the number of fire detection models considered in the decision-making process when labeling the new observation as “fire” or “non-fire”. Fig. 8 shows the effect of parameter w on the proposed algorithm in terms of average FSTA and FAR by setting the significance level $\alpha = 0.001$. If we utilize all the models simultaneously (i.e., $w = 3$), the models that are ineffective in detecting certain types of fire may result in delaying the fire detection time, even though lower FAR can be achieved. On the other hand, reducing the number of models in the decision-making process yields lower EFST with higher FAR. Thus, we recommend selecting reasonable w (e.g., $w = 1$) to achieve the best trade-off between FSTA and FAR. From a practical point of view, practitioners can choose appropriate w based on their engineering knowledge.

The parameter t_0 controls the number of past time points that the algorithm includes for each observation. If we set $t_0 = 1$, the decision-making is based only on the observation of current sensor measurements without using past information. On the other hand, increasing t_0 allows each observation to consider information from past sensor measurements. However, increasing t_0 may require a high computational time to perform the algorithm due to the increased number of wavelet-based features, making the algorithm less suitable for online monitoring. Therefore, the appropriate size of t_0 should be selected to monitor in real-time and include sensor measurements from the past in order to reduce the effect of the dynamic change and noise existing in the signal, which may result in false alarms. Table 8 presents FSTA and FAR of the proposed fire detection algorithm with the choice of t_0 under different

fire scenarios. Note that the numbers in bold denote the best performance for each fire scenario. Since the DWT requires t_0 to be a number with a power of 2, we choose $t_0 = 16, 32$, and 64 , and obtain the performance. As shown in the table, although the average FSTA of the proposed algorithm with $t_0 = 16$ is the smallest, the algorithm shows a better FSTA in only one scenario (i.e., Scenario 1) and yields higher FSTA in most of the other scenarios compared to other algorithms with longer t_0 . Moreover, notice that a fire alarm is raised (468 s in Scenario 1) when 10-consecutive time points are labeled as “fire” in the proposed algorithm. In other words, the algorithm with $t_0 = 16$ starts to label “fire” from 459 s which is less than the actual fire time of 467 s. This indicates that using a short time period utilizes less historical information, which may raise a false alarm that could cause needless evacuation and emergency plans. In contrast, increasing the parameter t_0 (e.g., $t_0 = 32$ and 64) results in low FSTA in most scenarios, and thus show robust performance regardless of different types of fire scenarios. By considering the computational time of the algorithm as an additional factor for the performance and median FSTA, therefore, we suggest selecting a reasonable value of t_0 (e.g., $t_0 = 32$) so that the overall performance of FSTA, FAR, and computational time can be enhanced.

Lastly, the parameter j_0 determines the lowest decomposition level. In addition, the size of the supporting interval, which contains sensor measurements for calculating wavelet coefficients, changes depending on j_0 . For instance, if the lowest decomposition level j_0 is set to 0, the signal with fixed time length $t_0 = 32$ can be represented by coefficients of the lowest resolution at scale $j_0 = 0$ (i.e., $c_{0,k}$ and $d_{0,k}$ which are

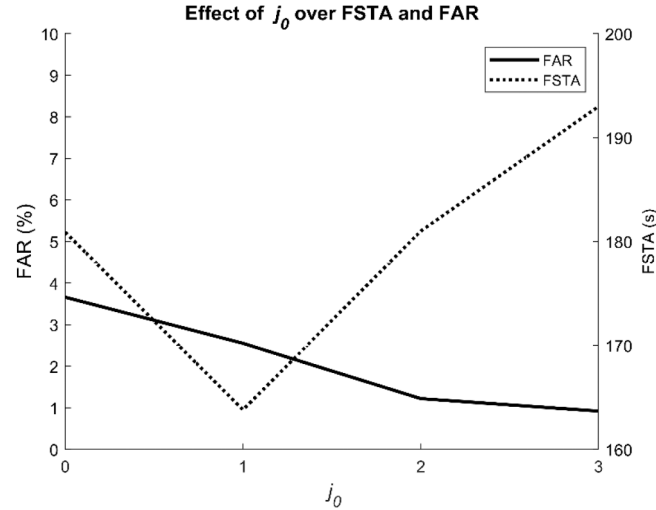


Fig. 9. Effect of the parameter j_0 on average FSTA and FAR.

Table 8

Performance of proposed approach with different time points.^a

Scenario #	TFST	WV-MMNN $t_0 = 16$			WV-MMNN ($t_0 = 32$)			WV-MMNN ($t_0 = 64$)		
		EFST (s)	FSTA (s)	FAR (%)	EFST (s)	FSTA (s)	FAR (%)	EFST (s)	FSTA (s)	FAR (%)
1	467	468	1	3.54	1205	738	0.00	1166	699	0.00
2	178	454	276	4.29	317	139	1.36	345	167	2.61
3	500	815	315	1.24	777	277	4.26	700	200	2.75
4	500	600	100	1.24	579	79	1.49	581	81	0.00
5	500	588	88	2.06	588	88	2.56	589	89	3.89
6	500	598	98	4.95	593	93	6.18	594	94	1.37
7	238	297	59	1.35	283	45	2.42	285	47	0.00
8	500	586	86	5.98	561	61	5.54	560	60	11.44
9	500	570	70	1.86	541	41	1.49	537	37	3.66
10	500	597	97	0.62	577	77	0.21	558	58	0.46
Median			92.50	1.96		83.50	1.96		85.00	1.99
Average			119.00	2.71		163.80	2.55		153.20	2.62

^a The numbers in bold denote the best performance for each fire scenario.

described by an interval containing 32 sensor measurements), and adding coefficients of higher resolutions at scale j (i.e., $d_{1,k}, d_{2,k}, d_{3,k}$ and $d_{4,k}$ which are obtained by intervals consisting of 16, 8, 4, and 2 neighboring measurements, respectively). In contrast, the size of intervals decreases as j_0 increases, and the number of neighboring sensor measurements utilized for wavelet coefficients decreases. Fig. 9 presents the effect of j_0 on the proposed algorithm in terms of average FSTA and FAR by setting $t_0 = 32$. Based on the figure, we suggest selecting a reasonable value of j_0 (e.g., $j_0 = 1$) which utilizes sufficient interval size to include enough measurement information in wavelet-based features so that the lowest FSTA with reasonable FAR can be achieved.

5. Case study with real-life fire data based on multi-sensor fusion system

In this section, the performance of the proposed approach is

demonstrated by applying it to real-life fire data obtained from the newly developed multi-sensor fusion system which is designed to provide various sensor information for monitoring different types of fires.

One of the major challenges in fire monitoring research is collecting real-life fire data for comparing the performance of different fire detectors. There have been several studies conducted to obtain fire sensor data from chemical sensor systems for decades in indoor buildings (Bukowski et al., 2008; Milarcik et al., 2008). However, a common drawback when comparing the performance of the fire detectors based on these studies is that fire starting time often varies from scenario to scenario due to uncontrolled experimental settings. In addition, only a limited number of sensor types and scenarios could be deployed in the performance comparison because some sensor measurements or sensor types are missing in some fire scenarios (Milarcik et al., 2008). Therefore, to overcome those drawbacks, we develop a novel multi-sensor fusion system which incorporates various chemical sensors, and

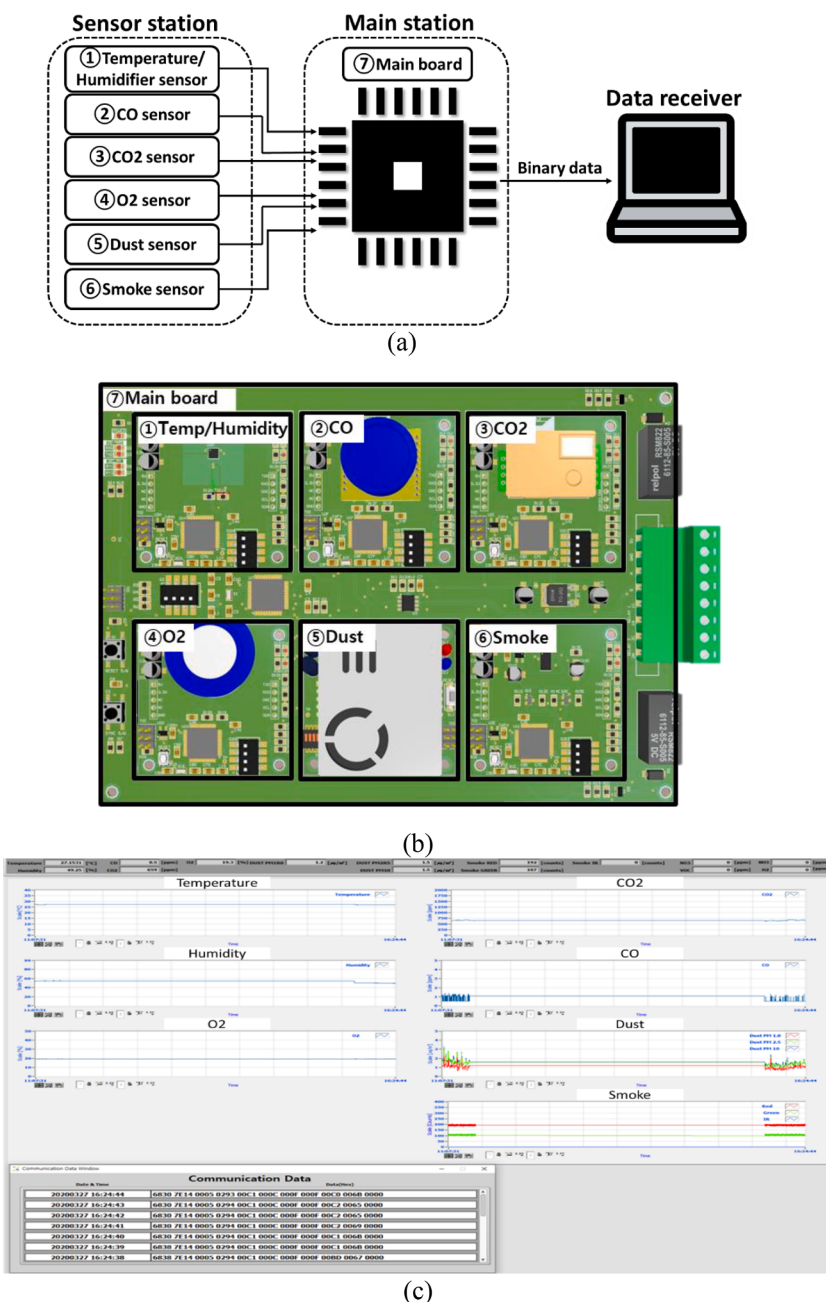


Fig. 10. (a) The conceptual architecture of the multi-sensor fusion system. (b) Illustration of the sensor and main station. (c) main screen of the data receiver.

collect a new fire sensor data from the controlled experimental design in order to validate the performance of the proposed and existing fire detection algorithms.

The multi-sensor fusion system consists of three parts: (i) sensor station, (ii) main station, and (iii) data receiver. The overall architecture of the system and illustration of the sensor and main station are shown in Fig. 10. The sensor station contains 6 sensor boards (i.e., temperature/humidity, CO, CO₂, O₂, dust, and smoke sensor boards) that measure 11 different sensor measurements, which are critical in monitoring fires. Details for sensor boards and their measurements are described in Fig. 11 and Table 9. The main station contains the main board that is responsible for collecting sensor data from multiple sensor boards. Collected data is then transmitted to the PC-based data receiver for further processing and analysis. The data receiver, equipped with LabView software, plays an essential role in reading, recording, and visualizing the collected sensor measurements. Fig. 10(c) presents the main screen of the LabView software, providing a display of the sensor measurements that are collected in real-time.

A total of 10 fire scenarios under different types (i.e., flaming, smoldering, and heating) of fire and non-fire scenario were considered for the purpose of the case study. Various materials, such as newspaper, textiles, sponges and plastic, etc., were used for the ignition, and TFST was settled to 300 s for all fire scenarios. Experiments took place in the test room specially designed to collect data used for fire monitoring using the proposed fire sensing system. Fig. 12(a) shows the inside view of the test room, and Fig. 12(b) describes fire experiments conducted in the testbed for data acquisition. During the experiment, 11 sensor measurements were collected at each second from the multi-sensor fire monitoring system. Table 10 summarizes the fire type, ignition materials, and TFST of each fire scenario. For each fire scenario, four experiments were repeatedly conducted to obtain a total of 40 experiments to be used in the case study. From the 40 experiments, 10 experiments that represent each fire scenario were utilized to obtain the best features for each fire type using the feature selection approach presented in Section 3.3, and the others were used for testing scenarios to evaluate the performance. To determine the decision boundary of the proposed WV-MMNN algorithm, a total of 1000 training observations, which are randomly selected from the non-fire scenario, are utilized using Algorithm 2.

Table 11 presents a comparison of the EFST, FSTA, and FAR of the proposed approach against other monitoring approaches described in

Table 9
Specification of sensor boards.

Sensor #	Sensor board (model name)	Sensor measurement	Measurement range	Measurement accuracy
1	Temperature/humidity (HDC1080)	Temperature Humidity	-40 ~ 125 °C 0 ~ 100%	± 0.2 °C ±2%
2	CO (ZE07 CO)	CO level	0 ~ 500 ppm	-
3	CO ₂ (MH Z19B)	CO ₂ level	0 ~ 5000 ppm	±(3%+50 ppm)
4	O ₂ (ZE03 O2)	O ₂ level	0 ~ 25%	±3.5%
5	Dust (PMS7003)	PM 1.0 dust intensity PM 2.5 dust intensity PM 10.0 dust intensity	0 ~ 500 g/m ³ (100 ~ 500 µg/m ³), ±10 µg/m ³ (0 ~ 100 µg/m ³)	±10%
6	Smoke (MAX30105)	ADC count of infrared ray LED ADC count of red LED ADC count of green LED	0 ~ 65536 count	-

ADC: Analog to digital converter, LED: Light-emitting diode, PM: Particulate matter.

Section 4.2. Note that average EFST, FSTA, and FAR are calculated by taking means of EFST, FSTA, and FAR for all experiments for each scenario. Among TBAs, TBA 1, which shares common sensors with our multi-sensor system, was chosen for the performance comparison. As shown in the table, the WV-MMNN algorithm outperforms the existing algorithms in terms of FSTA with reasonable FAR.

From experimental studies from both Section 4 and Section 5, we can draw a conclusion that the proposed approach is effective in monitoring different types of the fire in an early stage.

6. Discussion: future work and potential applications

There are a number of potential avenues to improve the proposed fire detection algorithm. One of the limitations of the proposed approach is that although wavelet-based features consider temporal dependency within the signal, they do not take into account the correlation between

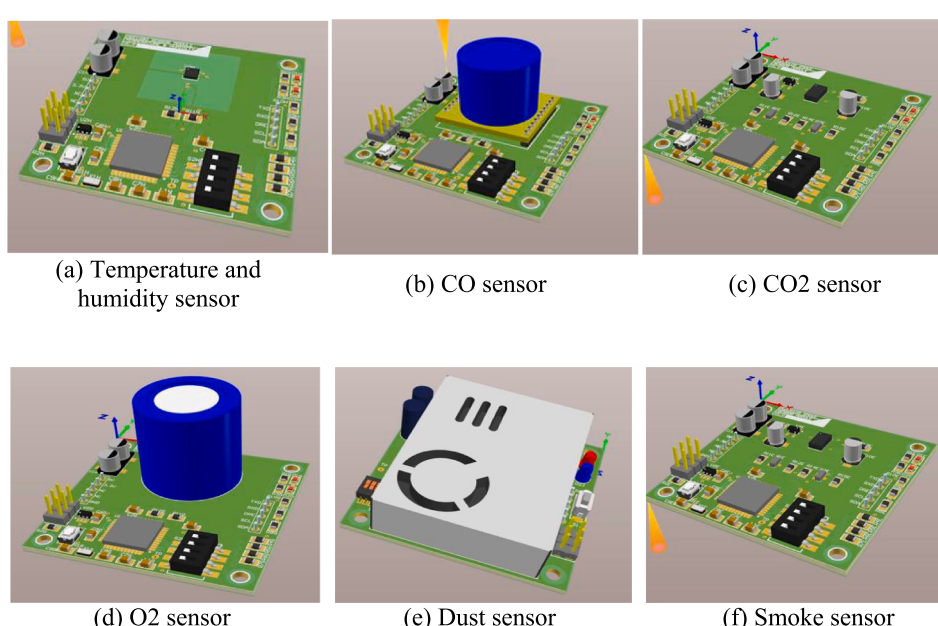


Fig. 11. Illustration of sensor boards.

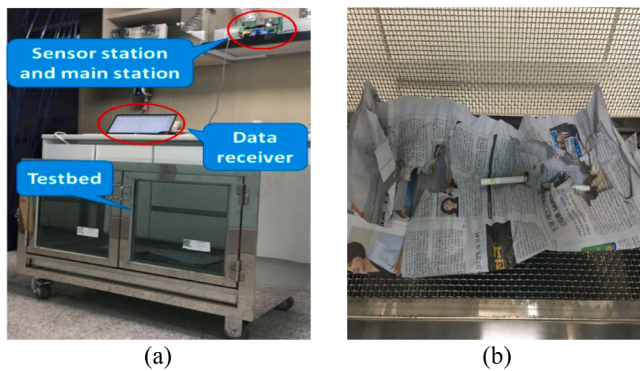


Fig. 12. (a) Inside view of the test room. (b) Examples of fire experiments conducted for data acquisition.

Table 10
Description of experiment scenarios obtained through the multi-sensor fusion system.

Scenario #	Fire type	Fire ignition material	TFST (s)
1	Heating	Food	300
2	Flaming	Polyurethane	300
3	Flaming	Newspaper	300
4	Smoldering	Newspaper	300
5	Flaming	Plastic	300
6	Flaming	Sponge	300
7	Flaming	Textile	300
8	Smoldering and flaming	Paper and paper towel	300
9	Flaming	Wooden chopsticks	300
10	Flaming	Wooden piece	300
11	Non-fire	—	—

Table 11
Performance of existing and proposed fire detection algorithm on real-life fire scenarios.^a

Scenario #	TBA 1			Q-statistic			T^2 -statistic		
	Average EFST (s)	Average FSTA (s)	Average FAR (%)	Average EFST (s)	Average FSTA (s)	Average FAR (%)	Average EFST (s)	Average FSTA (s)	Average FAR (%)
1	406	106	0.00	905	605	0.00	503	203	0.00
2	182	227	66.67	902	602	0.00	285	157	18.78
3	48	252	79.48	568	268	0.00	259	132	2.24
4	390	263	30.35	1203	903	0.00	447	147	0.00
5	277	149	33.33	902	602	0.00	412	112	0.00
6	388	88	0.00	903	603	0.00	152	198	66.67
7	193	239	66.67	902	602	0.00	290	162	10.82
8	41	259	100.00	905	605	0.00	515	215	0.00
9	41	259	100.00	924	624	0.00	367	93	3.86
10	171	216	66.67	1070	770	0.00	375	75	0.00
Median	233.00	66.67	—	—	604.00	0.00	—	152.00	1.12
Average	205.73	54.32	—	—	618.33	0.00	—	149.27	10.24
Scenario #	WV-PNN			LSTM			WV-MMNN		
	Average EFST (s)	Average FSTA (s)	Average FAR (%)	Average EFST (s)	Average FSTA (s)	Average FAR (%)	Average EFST (s)	Average FSTA (s)	Average FAR (%)
1	221	88	22.26	140	186	66.67	453	153	0.12
2	68	232	62.94	152	197	66.67	410	110	0.00
3	447	278	17.91	250	123	1.37	346	46	0.12
4	176	124	21.52	395	95	0.00	470	170	0.00
5	902	602	0.00	41	259	100.00	392	92	0.00
6	41	259	99.88	151	196	66.67	361	61	0.00
7	274	147	31.22	392	92	0.00	391	91	0.12
8	245	286	42.66	254	127	2.61	516	216	0.00
9	613	313	3.36	167	207	35.82	393	93	1.87
10	504	238	3.48	151	196	66.67	370	70	0.00
Median	248.50	21.89	—	—	191.00	51.25	—	92.50	0.00
Average	256.80	30.52	—	—	167.83	40.65	—	110.23	0.22

^a The numbers in bold indicate the best FSTA performance.

two different fire sensor signals. It is possible that a number of different sensors that react to certain fire types may be correlated to each other, and this may provide crucial information to detect the fire in an early stage. Therefore, we intend to improve our research to develop new features that can capture the correlation between fire sensor signals and apply them to fire detection algorithms. In addition, the proposed fire detection approach can be extended to find the location of the fire once the observed sensor measurements are identified as “fire” when sensors are installed at multiple locations. In our approach, if sensors are installed at multiple locations, the selected wavelet-based features are applied to sensor measurements at each location to obtain the new input dataset. If the current observation is classified as “fire”, we can perform WV-MMNN to the current observation at each location and calculate the local NN distances. Since the local NN distance of the observation at the fire ignition location yields a high value compared to others, it can be potentially utilized to identify the fire location.

It is important to note that the proposed multi-sensor fusion system can be improved by leveraging state-of-the-art technologies. Recently, there has been growing adoption of technologies such as the Internet of Things (IoT), digital twin technology, and cyber-physical systems in the domain of firefighting (Hamins et al., 2015; Sungheetha & Sharma, 2020; Zhang et al., 2022), and such technologies hold the potential for further exploration and advancement of the proposed system. IoT sensors have been strategically installed throughout the indoor building to monitor real-time sensor information related to fire detection, such as smoke, light, humidity, and temperature (Sungheetha & Sharma, 2020; Zhang et al., 2022). The sensors collect a vast amount of data in real-time and transmit it wirelessly to cloud storage systems that are capable of handling large volumes of information. By utilizing this data and employing the proposed algorithm, a higher level of accuracy could be achieved in detecting various types of fire. Moreover, rather than using the sensor measurements from simple fire testing, we can incorporate a more sophisticated digital twin structure that simulates historical fire disasters. This advanced feature enables the system to

generate more precise and realistic sensor information, which can potentially improve the overall performance of the system. It is also possible to develop a user interface based on the smartphone that enables individuals to monitor sensor data and receive real-time fire alarms, allowing a cyber-physical interaction and empowering users with immediate information and response capabilities. Lastly, instead of relying solely on a chemical sensor system, the proposed multi-sensor fusion system has the potential to improve the overall performance by incorporating video sensor systems. For instance, one possible enhancement includes incorporating thermographic cameras, which are popularly utilized across various industries, including building inspections, electrical maintenance, industrial processes, and firefighting (Bhattarai & Martinez-Ramon, 2020; Glowacz, 2022, 2023; Li et al., 2022). The thermographic camera produces real-time thermal images that can offer the advantage of temperature visualization and the detection of hidden or potential risks. In the context of fire monitoring, thermal images play a crucial role in enabling the system to detect the presence of a fire by capturing the infrared radiation emitted by heat sources. By utilizing the visual images captured by the camera, the system can significantly reduce false alarms and detect hidden fires that may not be visible to the naked eye.

7. Conclusions

In this study, we developed a novel wavelet-based fire detection algorithm that utilizes various sensor information using wavelet multi-resolution analysis. Wavelet-based features effective in detecting fires were extracted, and features that can clearly distinguish between fire and non-fire conditions were selected by considering different types of fire. In addition, the WV-MMNN was proposed to effectively utilize selected features and construct multiple fire detectors that are sensitive in monitoring various types of fire. Lastly, we developed a novel fire sensing system that combines a variety of chemical sensors which are effective in fire monitoring. Then, real-life fire sensor data from various fire scenarios are collected from the multi-sensor fusion system under controlled experiments to analyze the performance of the proposed and existing fire detection algorithms. Experimental results with public and real-world fire datasets indicate that the wavelet-based fire detection algorithm outperforms other existing approaches in terms of lower average FSTA (163.80 and 110.23) and median FSTA (83.50 and 92.50) with reasonable average FAR (2.55 and 0.22) and median FAR (1.95 and 0.00), respectively, attesting that the proposed approach reliably achieves high performance in detecting fires, regardless of the variability in fire types.

The proposed research can bring several additional advantages to the fire research society. The dataset collected from the new fire sensing system allows researchers to carry out developing more robust and effective fire detection algorithms since the new dataset overcomes the limitations of existing datasets by having unified experiment settings for all different fire types as well as using high-quality sensor devices that have no interruption in collecting sensor measurements that eliminates missing values in the dataset. Furthermore, the collected dataset includes more ignition sources that closely resemble indoor fires. A broader range of ignition sources enables society to conduct a comprehensive analysis of fire behaviors that can ultimately lead to improving existing fire detection algorithms and enhancing fire mitigation strategies. Finally, the general society can benefit from the proposed fire detection system. Developing an accurate and reliable fire detection system can enhance overall safety by enabling prompt response and evacuation, effectively reducing potential damage to assets, injuries, and fatalities.

CRediT authorship contribution statement

Jaeseung Baek: Methodology, Software, Validation, Formal analysis, Writing – original draft, Writing – review & editing, Visualization,

Investigation. **Taha J. Alhindi:** Methodology, Software, Validation, Investigation, Writing – original draft, Visualization. **Young-Seon Jeong:** Writing – review & editing, Conceptualization, Methodology. **Myong K. Jeong:** Writing – review & editing, Supervision, Conceptualization, Methodology, Funding acquisition. **Seongho Seo:** Resources, Funding acquisition, Data curation. **Jongseok Kang:** Resources, Funding acquisition, Data curation. **We Shim:** Resources, Funding acquisition, Data curation. **Yoseob Heo:** Resources, Funding acquisition, Data curation.

Declaration of Competing Interest

The authors declare that they have no known competing financial interests or personal relationships that could have appeared to influence the work reported in this paper.

Data availability

Data will be made available on request.

Acknowledgments

The authors thank the reviewers for the helpful and constructive comments that greatly contributed to the improvement of the paper. This work was supported in part by the Safety Technology Commercialization Platform Construction Project (No. P0003951) with fund of the South Korean Ministry of Trade, Industry and Energy. In addition, this work was partially supported by National Research Foundation of Republic of Korea Grant (NRF-2022R1F1A1063174).

References

- Baek, J., Alhindi, T. J., Jeong, Y.-S., Jeong, M. K., Seo, S., Kang, J., ... Heo, Y. (2021). Real-time fire detection system based on dynamic time warping of multichannel sensor networks. *Fire Safety Journal*, 123, Article 103364.
- Baidari, I., & Honnigkoll, N. (2021). Bhattacharyya distance based concept drift detection method for evolving data stream. *Expert Systems with Applications*, 183, Article 115303.
- Benzekri, W., El Moussati, A., Moussaoui, O., & Berrajaa, M. (2020). Early forest fire detection system using wireless sensor network and deep learning. *International Journal of Advanced Computer Science and Applications*, 11(5).
- Bertolini, M., Mezzogori, D., Neroni, M., & Zammori, F. (2021). Machine Learning for industrial applications: A comprehensive literature review. *Expert Systems with Applications*, 175, Article 114820.
- Bhattarai, M., & Martinez-Ramon, M. (2020). A deep learning framework for detection of targets in thermal images to improve firefighting. *IEEE Access*, 8, 88308–88321.
- Bukowski, R. W., Peacock, R. D., Averill, J. D., Cleary, T. G., Bryner, N. P., Walton, W. D., & Reneke, P. A. (2008). Performance of home smoke alarms. *NIST Technical Note*, 1455.
- Cestari, L. A., Worrell, C., & Milke, J. A. (2005). Advanced fire detection algorithms using data from the home smoke detector project. *Fire Safety Journal*, 40(1), 1–28.
- Chaoxia, C., Shang, W., & Zhang, F. (2020). Information-guided flame detection based on faster R-CNN. *IEEE Access*, 8, 58923–58932.
- Chen, S.-J., Hovde, D. C., Peterson, K. A., & Marshall, A. W. (2007). Fire detection using smoke and gas sensors. *Fire Safety Journal*, 42(8), 507–515.
- Cleary, T. G. (2011). An analysis of the performance of smoke alarms. *Fire Safety Science*, 10, 823–836.
- Croux, C., & Ruiz-Gazen, A. (2005). High breakdown estimators for principal components: The projection-pursuit approach revisited. *Journal of Multivariate Analysis*, 95(1), 206–226.
- Dasari, P., Reddy, G. K. J., & Gudipalli, A. (2020). Forest fire detection using wireless sensor networks. *International Journal on Smart Sensing and Intelligent Systems*, 13(1), 1–8.
- Dey, P., Chaulya, S., & Kumar, S. (2021). Hybrid CNN-LSTM and IoT-based coal mine hazards monitoring and prediction system. *Process Safety and Environmental Protection*, 152, 249–263.
- Dinaburg, J., & Guttuk, D. T. (2011). Home Cooking Fire. Mitigation: Technology Assessment. Final Report.
- Fonollosa, J., Solórzano, A., & Marco, S. (2018). Chemical sensor systems and associated algorithms for fire detection: A review. *Sensors*, 18(2), 1–39.
- Gaur, A., Singh, A., Kumar, A., Kulkarni, K. S., Lala, S., Kapoor, K., ... Mukhopadhyay, S. C. (2019). Fire sensing technologies: A review. *IEEE Sensors Journal*, 19(9), 3191–3202.
- Glowacz, A. (2022). Thermographic fault diagnosis of shaft of BLDC motor. *Sensors*, 22 (21), 8537.

- Glowacz, A. (2023). Thermographic fault diagnosis of electrical faults of commutator and induction motors. *Engineering Applications of Artificial Intelligence*, 121, Article 105962.
- Gottuk, D. T., Peatross, M. J., Roby, R. J., & Beyler, C. L. (2002). Advanced fire detection using multi-signature alarm algorithms. *Fire Safety Journal*, 37(4), 381–394.
- Gu, X., Akoglu, L., & Rinaldo, A. (2019). Statistical analysis of nearest neighbor methods for anomaly detection. *Advances in Neural Information Processing Systems*, 32.
- Hamins, A. P., Bryner, N. P., Jones, A. W., & Koepke, G. H. (2015). Research roadmap for smart fire fighting.
- Hilal, W., Gadsden, S. A., & Yawney, J. (2021). A review of anomaly detection techniques and applications in financial fraud. *Expert Systems with Applications*, 116429.
- Huang, L., Liu, G., Wang, Y., Yuan, H., & Chen, T. (2022). Fire detection in video surveillances using convolutional neural networks and wavelet transform. *Engineering Applications of Artificial Intelligence*, 110, Article 104737.
- Ji, R. D., Hammond, M. H., Williams, F. W., & Rose-Pehrsson, S. L. (2003). Multivariate statistical process control for continuous monitoring of networked early warning fire detection (EWFD) systems. *Sensors and Actuators B: Chemical*, 93(1–3), 107–116.
- Kailath, T. (1967). The divergence and Bhattacharyya distance measures in signal selection. *IEEE Transactions on Communication Technology*, 15(1), 52–60.
- Kumar, S., Janet, B., & Neelakantan, S. (2022). Identification of malware families using stacking of textural features and machine learning. *Expert Systems with Applications*, 208, Article 118073.
- Kwak, B. I., Han, M. L., & Kim, H. K. (2020). Driver identification based on wavelet transform using driving patterns. *IEEE Transactions on Industrial Informatics*, 17(4), 2400–2410.
- Li, J., Yan, B., Zhang, M., Zhang, J., Jin, B., Wang, Y., & Wang, D. (2019). Long-range raman distributed fiber temperature sensor with early warning model for fire detection and prevention. *IEEE Sensors Journal*, 19(10), 3711–3717.
- Li, S., Wang, Y., Feng, C., Zhang, D., Li, H., Huang, W., & Shi, L. (2022). A Thermal Imaging Flame-Detection Model for Firefighting Robot Based on YOLOv4-F Model. *Fire*, 5(5), 172.
- Lin, G., Zhang, Y., Xu, G., & Zhang, Q. (2019). Smoke detection on video sequences using 3D convolutional neural networks. *Fire Technology*, 55(5), 1827–1847.
- Majid, S., Alenezi, F., Masood, S., Ahmad, M., Gündüz, E. S., & Polat, K. (2022). Attention based CNN model for fire detection and localization in real-world images. *Expert Systems with Applications*, 189, Article 116114.
- Milarcik, E., Olenick, S., & Roby, R. (2008). A relative time analysis of the performance of residential smoke detection technologies. *Fire Technology*, 44(4), 337–349.
- Milke, J. A., Hulcher, M. E., Worrell, C. L., Gottuk, D. T., & Williams, F. W. (2003). Investigation of multi-sensor algorithms for fire detection. *Fire Technology*, 39(4), 363–382.
- Mohebali, B., Tahmassebi, A., Meyer-Baese, A., & Gandomi, A. H. (2020). Probabilistic neural networks: A brief overview of theory, implementation, and application. *Handbook of probabilistic models*, 347–367.
- Muduli, L., Mishra, D. P., & Jana, P. K. (2019). Optimized fuzzy logic-based fire monitoring in underground coal mines: Binary particle swarm optimization approach. *IEEE Systems Journal*, 1–8.
- Nazir, A., Mosleh, H., Takruri, M., Jallad, A.-H., & Alhebsi, H. (2022). Early fire detection: A new indoor laboratory dataset and data distribution analysis. *Fire*, 5(1), 11.
- Oyedare, T., & Park, J.-M.-J. (2019). Estimating the required training dataset size for transmitter classification using deep learning. *2019 IEEE International Symposium on Dynamic Spectrum Access Networks (DySPAN)*.
- Pincott, J., Tien, P. W., Wei, S., & Calautit, J. K. (2022). Indoor fire detection utilizing computer vision-based strategies. *Journal of Building Engineering*, 61, Article 105154.
- Santos, M. A., Christensen, E. G., Yang, J., & Rein, G. (2019). Review of the transition from smouldering to flaming combustion in wildfires. *Frontiers in Mechanical Engineering*, 5, 49.
- B.E. Shelby Hall Fire Loss in The United States. National Fire Protection Association <https://www.nfpa.org/News-and-Research/Data-research-and-tools/US-Fire-Problem/Fire-loss-in-the-United-States> 2022 Retrieved 4/8/2023 from.
- Sousa, M. J., Moutinho, A., & Almeida, M. (2019). Classification of potential fire outbreaks: A fuzzy modeling approach based on thermal images. *Expert Systems with Applications*, 129, 216–232.
- Soydaner, D. (2020). A comparison of optimization algorithms for deep learning. *International Journal of Pattern Recognition and Artificial Intelligence*, 34(13), 2052013.
- Stauffer, E., Dolan, J. A., & Newman, R. (2007). *Fire debris analysis*. Academic Press.
- Sungeetha, A., & Sharma, R. (2020). Real time monitoring and fire detection using internet of things and cloud based drones. *Journal of Soft Computing Paradigm (JSCP)*, 2(03), 168–174.
- Tao, H., & Duan, Q. (2023). An adaptive frame selection network with enhanced dilated convolution for video smoke recognition. *Expert Systems with Applications*, 215, Article 119371.
- Theodoridis, S., & Koutroumbas, K. (2009). *Pattern recognition*. Elsevier Science & Technology.
- Théodore, R., Denis, D., Chateau, T., Fremont, V., & Checchin, P. (2021). A deep learning approach for LiDAR resolution-agnostic object detection. *IEEE Transactions on Intelligent Transportation Systems*, 23(9), 14582–14593.
- Vidakovic, B. (2009). *Statistical modeling by wavelets* (Vol. 503). John Wiley & Sons.
- Wang, X.-G., Lo, S.-M., & Zhang, H.-P. (2013). Influence of feature extraction duration and step size on ANN based multisensor fire detection performance. *Procedia Engineering*, 52, 413–421.
- Wu, X., Park, Y., Li, A., Huang, X., Xiao, F., & Usmani, A. (2021). Smart detection of fire source in tunnel based on the numerical database and artificial intelligence. *Fire Technology*, 57, 657–682.
- Xu, Z., Guo, Y., & Saleh, J. H. (2021). Advances toward the next generation fire detection: Deep LSTM variational autoencoder for improved sensitivity and reliability. *IEEE Access*, 9, 30636–30653.
- Zhang, T., Wang, Z., Zeng, Y., Wu, X., Huang, X., & Xiao, F. (2022). Building Artificial Intelligence Digital Fire (AID-Fire) system: A real-scale demonstration. *Journal of Building Engineering*, 62, Article 105363.
- Zheng, D., Wang, Y., & Wang, Y. (2015). Intelligent monitoring system for home based on FRBF neural network. *International Journal of Smart Home*, 9(2), 207–218.